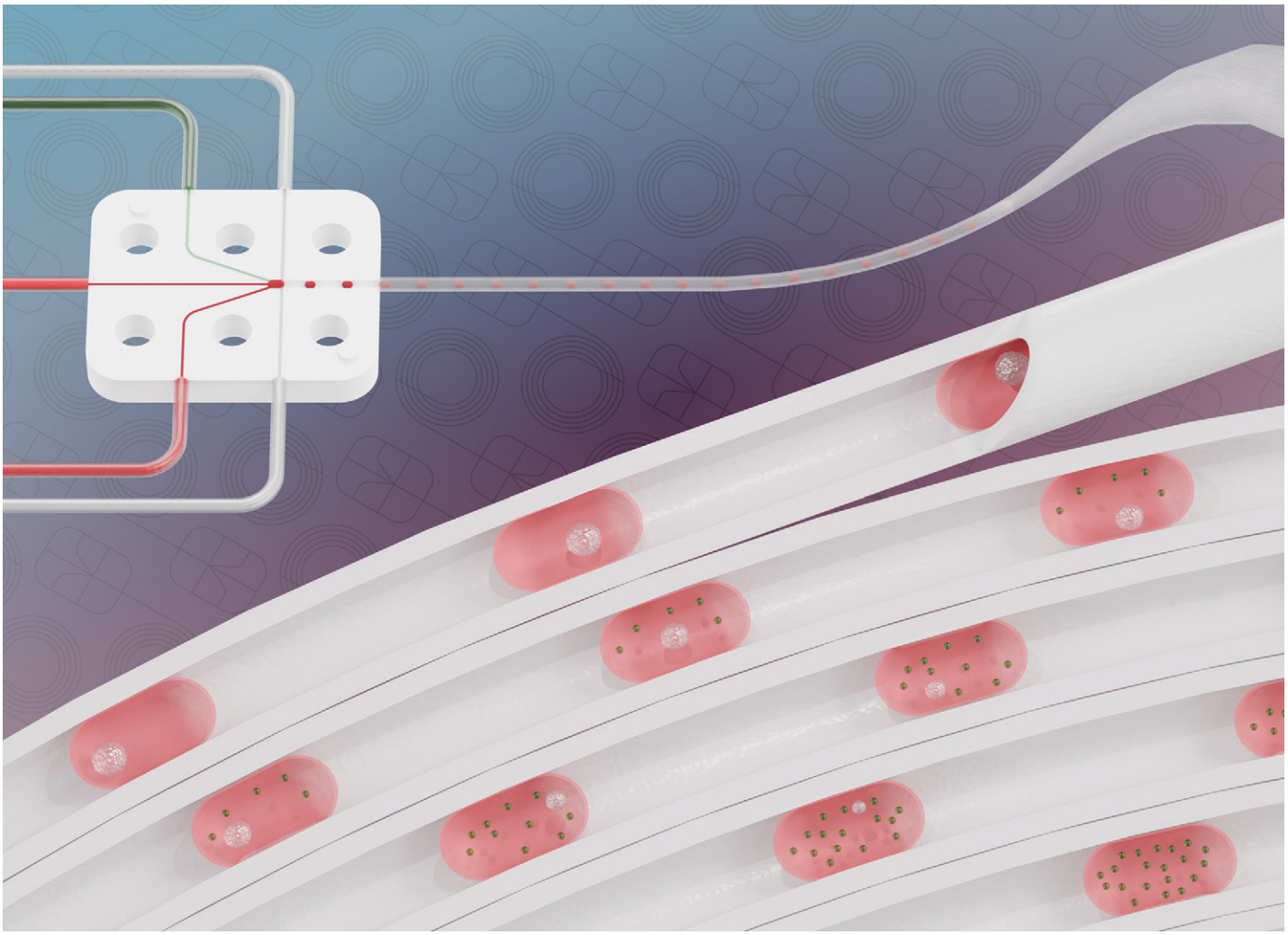

Showcasing work from the research group of Dr. Karen Lemke's laboratory, Institute for Bioprocessing and Analytical Measurement Techniques e.V., Thuringia, Germany.

Droplet-based cell viability assay for analysis of spheroid formation, proliferation and high-resolution IC_{50} profiling

The highly flexible droplet-based *pipe-based bioreactors (pbb)* technology enables the CellTiter-Blue® cell viability assay for drug screening of 3D cell cultures. The precise adjustment of a continuous flow rate profile allows the reproducible generation of droplets with defined cell concentrations and linearly increasing drug concentrations. A time-efficient and high-resolution determination of the IC_{50} value for HEK-293 spheroids is realized. In summary, the *pbb* technology surpasses the state of the art and proves to be a useful tool for disease modelling. Image designed and illustrated by Robert Römer (iba e.V.).

As featured in:

See Mario Saupe *et al.*, *Lab Chip*, 2025, **25**, 6138.

ROYAL SOCIETY OF CHEMISTRY

rsc.li/loc

Registered charity number: 207890

Lab on a Chip

PAPER

View Article Online
View Journal | View Issue

Cite this: *Lab Chip*, 2025, **25**, 6138

Droplet-based cell viability assay for analysis of spheroid formation, proliferation and high-resolution IC_{50} profiling

Mario Saupe, *[ab] Stefan Wiedemeier,[a] Franziska Moll, [a] J. Michael Köhler, [b] Doris Heinrich[ab] and Karen Lemke[a]

Three-dimensional (3D) cell cultures or samples generated from biopsies are typically used as patient-specific *in vitro* models. As 3D cell cultures form cell–cell and cell–matrix interactions and mimic the *in vivo* situation better compared to monolayer cultures, they provide more reliable data for drug screening applications. In the field of drug screening, microfluidics is moving to the forefront for testing the efficacy of drugs, as measured by IC_{50} values. Droplet-based microfluidics not only shares the advantages of well plate-based systems but also those that go beyond. The high-throughput character of droplet-based microfluidics enables the generation of hundreds of droplets per minute, with smaller volumes than in well plate-based systems. The high level of automation and the closed character of such systems permit a higher reproducibility of the generated data, as the well-known problem of evaporation in well plates is negligible. In this study, a modular droplet-based microfluidic platform is introduced that facilitates the formation of 3D cell cultures. For assessing cell viability in spheroids of the human embryonic kidney cell line, HEK-293, a resazurin-based CellTiter-Blue® assay was established on a droplet-based platform. Here, the *pipe based bioreactors* (*pbb*) technology was used to create a continuous drug gradient, enabling the realisation of 290 concentration levels within a single droplet sequence to determine high-resolution IC_{50} values. Consequently, the *pbb* technology exceeds the state of the art, as only discrete concentrations of drugs are investigated in well plate-based systems. DMSO was used for drug testing experiments, as drugs are typically dissolved in it. As it is important that healthy cells are not affected by the drug or its solvents, the influence of DMSO was examined. Overall, the presented platform not only offers a robust and precise tool for validating drug efficacy using 3D cell cultures but also provides the basis for developing innovative therapies across a wide range of diseases. The modular design of the *pbb* platform provides the flexibility to address a variety of biomedical applications, ultimately accelerating personalized medicine to deliver better outcomes for patients.

Received 20th May 2025,
Accepted 17th July 2025

DOI: 10.1039/d5lc00495k

rsc.li/loc

1. Introduction

The growing focus on individualized medical approaches using 3D cell cultures, such as scaffold-based or scaffold-free models, offers several advantages over traditional two-dimensional models.[1] As these culture methods more closely mimic the *in vivo* situation, they enhance the probability of successful pharmacological studies. Consequently, the use of 3D cell cultures has the potential to reduce costs.[2] Furthermore, 3D cell cultures represent a valuable compromise between monolayer cultures and animal models, with the additional benefit of reducing the number of animals used in research.[3] They provide the opportunity to investigate models that exhibit both cell–cell and cell–matrix interactions at high cell densities.[4]

Microfluidic systems are well-suited for forming such 3D cell cultures, both in perfusion systems and using co-cultures.[5] Numerous applications have been successfully established in droplet-based microfluidic technologies.[6–9] This technology offers numerous advantages comparable to those of well plate-based systems, such as its high-throughput capabilities.[10,11] As a result, it is possible to generate high sample numbers in both technologies, leading to an elevated statistical confidence.

Furthermore, they are highly automated, resulting in excellent reproducibility. In the case of droplet-based microfluidics, this is possible without the need for laboratory space-consuming pipetting robots. Furthermore, droplet-based systems offer additional advantages that

[a] *Institute for Bioprocessing and Analytical Measurement Techniques e.V, Rosenhof, 37308 Heilbad Heiligenstadt, Germany. E-mail: Mario.Saupe@iba-heiligenstadt.de*
[b] *Faculty of Mathematics and Natural Sciences, Technische Universität Ilmenau, Ehrenbergstr. 29, 98693 Ilmenau, Germany*

surpass well plate technology. For instance, due to the closed nature of such systems, well-known problems of evaporation are negligible. Also, as the bioreactors consist of smaller volumes, lower amounts of medium, drugs, and dyes are used, which demonstrates the high sustainability of droplet-based approaches. In contrast to other systems, the presented *pipe based bioreactors* (*pbb*) technology additionally allows for high-definition linear adjustment of drug concentrations to realize high-resolution IC_{50} values.

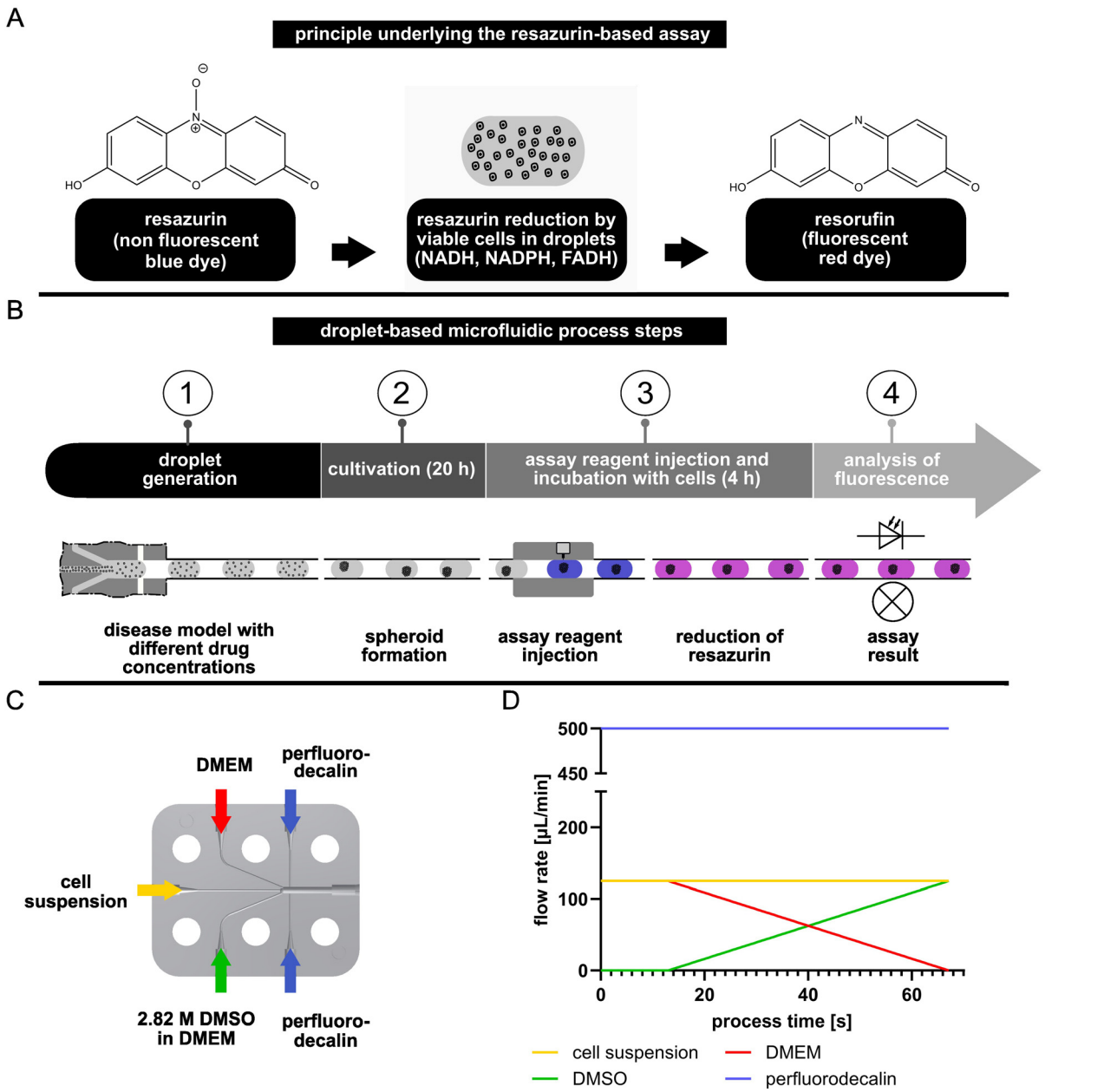

Fig. 1 Schematic overview of the resazurin-based cell viability assay and microfluidic droplet generation process. (A) Principle underlying the chemical reaction of the resazurin-based cell viability assay, showing resazurin reduction to resorufin by viable cells in droplets. (B) Sequential microfluidic steps involved in the resazurin-based viability assay, along with the associated modules of the droplet-based microfluidic platform. (1) Droplet generation within the gradient module (GM) for initial mixing of defined cell counts per droplet with linear adaptable drug concentrations of DMSO. (2) Cultivation of adherent cell lines using the storage module (SM) and spheroid formation during 20 h of incubation. (3) Injection of the cell viability assay reagent by the conditioning module (CM) and reduction to the fluorescent resorufin during a 4 h incubation period. (4) Analysis of fluorescence intensities in the droplets depending on the viable cell count using the analysis module (AM). (C) Mixer concept of the gradient module and connection of the fluids for realizing the resazurin-based assay in droplet-based microfluidics. The yellow channel serves as the inlet for homogenous guidance of a cell suspension. The green and red channels serve as inlets for cell culture media as well as drugs, facilitating continuous mixing of them. Through the blue channel, the continuous oil phase is pumped to generate droplets. (D) Continuous flow rate profile for high-resolution linear drug concentration adjustment with reproducible cell counts per droplet in a single sequence.

As not all drugs that target cancer cells are effective against every cancer type, and some cancers may even be resistant to first-line therapies, new treatment strategies are necessary. Different therapeutics developed for other diseases are now being evaluated for their potential effects on cancer cells.[12,13] The development of new drugs is of particular importance in the context of cancer, given the lack of available therapies that offer complete cures for some cancer types on the one hand and the lowest toxicity to healthy cells on the other hand.[14–16] For example, glioblastoma and pancreatic cancers deliver poor prognoses and short survival periods for patients.[17] The main reasons for this are the inability of drugs to cross the blood–brain barrier in the case of glioblastoma, drug resistance in pancreatic cancer, and the recurring late diagnoses of these diseases overall.[18,19]

The determination of IC_{50} values is commonly used as an informative measure of a drug's efficacy to develop therapeutic regimens for patients with particular diseases.[20] The value indicates the concentration of a drug at which 50% of a biological process is inhibited. The most common methods for evaluating IC_{50} values are cell viability assays, such as the MTT assay, the CellTiterGlo assay, and the CellTiter-Blue® assay. These assays are based on measurements of absorbance, luminescence, or fluorescence. In all cases, the optical signal correlates with the concentration of viable cells; the greater the intensity, the higher the concentration of viable cells is.[21–23]

In this study, the resazurin-based CellTiter-Blue® cell viability assay was adapted for use on a droplet-based microfluidic platform to determine IC_{50} values. The assay uses resazurin, a non-fluorescent blue dye, which viable cells can reduce to resorufin, a fluorescent red dye (see Fig. 1A). This results from cellular metabolic processes involving NADH, NADPH, FADH, FMNH, and cytochromes.[24] The fluorescence shift is a more sensitive method of measurement than absorbance.[25] Here, the modular droplet-based microfluidic platform (*pbb* technology) was used as a tool to realize a continuous drug gradient within a single droplet sequence. In this context, a standard operating procedure (SOP) was developed using adherent HEK-293 cells to form 3D cell structures by self-assembly within droplets. The *pbb* platform includes a series of varying modules, each with a specific function to realize defined microfluidic process steps. All modules have been previously described and characterized.[26] For the establishment of the resazurin-based assay, further characterization steps using the gradient module (GM) were necessary. These steps were implemented to realize a novel approach for the high-resolution adjustment of defined dimethyl sulfoxide (DMSO) concentrations with high precision. This approach enables the adjustment of drug concentrations in consecutive droplets in small steps.

2. Materials and methods

Solutions and chemicals

Cell cultivation. The dispersed phase for all experiments was DMEM cell culture medium (D5523, Sigma-Aldrich Chemie GmbH, Taufkirchen, Germany), supplemented with 5.5 g L^{-1} D-glucose (G7021, Sigma-Aldrich Chemie GmbH, Taufkirchen, Germany), 2 mM L-glutamine (G8540, Sigma-Aldrich Chemie GmbH, Taufkirchen, Germany), 100 U penicillin/100 μg mL^{-1} streptomycin (15140-122, Life Technologies, Darmstadt, Germany), and 10% [v/v] fetal calf serum (FCS) (S1810-500, BioWest, Nuaille, France).

For cell experiments, HEK-293 cells (ACC 305, DSMZ – German collection of Microorganisms and Cell Cultures GmbH, Braunschweig, Germany) were used as a suspension in the already described DMEM cell culture medium.

As a continuous phase, perfluorodecalin (PFD) (ALFA AESAR, Karlsruhe, Germany, A18288) was used in all experiments.

The resorufin sodium salt powder (424455-1G, Sigma-Aldrich Chemie GmbH, Taufkirchen, Germany) was dissolved in fully supplemented DMEM to a final concentration of 100 μg mL^{-1}.

Sterilization protocol for the droplet-based microfluidic platform for cell experiments

Prior to each experiment, the mixing module (MixM) was disinfected in an 80% [v/v] ethanol bath for 20 minutes and subsequently dried in a sterile hood. All microfluidic modules were plasma-functionalized (Pico-RF-μW-PC-c, Diener Electronics GmbH + Co. KG, Ebhausen, Germany) as previously described[26] and assembled immediately. All tubes and connectors were sterilized by autoclaving (15 min, 121 °C, Varioklav 135S, HP Labortechnik GmbH, Oberschleißheim, Germany). The whole platform was assembled under sterile conditions, and the PFD was filtered sterile (pore size, 0.45 μm) prior to use.

SOP to realize the droplet-based cell viability assay

The process steps of the CellTiter-Blue® cell viability assay were transferred to the droplet-based *pbb* platform (see Fig. S1A).[26] To achieve a homogeneous distribution of cells within the droplets, a mixing module (MixM) was used as the initial component of each drug screening procedure. The GM (see Fig. S1B) was used to generate droplets with defined cell counts and a continuous drug gradient in a single droplet sequence, in combination with a continuous flow rate profile. Here, the GM was arranged vertically for better spheroid reproducibility. The droplet module (DM) enabled spacing between droplets within a sequence. The conditioning module (CM) facilitated the active automated injection of defined volumes of the CellTiter-Blue® reagent into an existing droplet sequence (see Fig. S1C). Fluorescence intensities of the droplets were determined using the analysis module (AM) (see Fig. S1D), which is connected to a light source (ILP-2, EVIDENT Germany GmbH, Hamburg, Germany) and a spectrometer (SILVER-Nova, StellarNet Inc., Tampa, FL, USA) *via* optical fibres. Finally, for proliferation experiments, a storage module (SM) was used in combination with a microscopy module (MicM) for microscopic analysis.

Evaluating the reproducibility of droplet generation using a continuous flow rate profile

The QMixElements software (Cetoni GmbH, Korbußen, Germany) was used to create a flow rate profile for continuous adjustment of drug concentrations in the droplets (see Fig. 1D). The experiment was performed using a Nemesys syringe pump (Cetoni GmbH, Korbußen, Germany). Maintaining a constant flow rate of 125 μL min^{-1} (yellow channel, Fig. 1C), using a 10 mL syringe (SETonic GmbH, Ilmenau, Germany). During the experiment, the drug flow rate was continuously increased, from 0 μL min^{-1} to 125 μL min^{-1} (green channel, Fig. 1C, 2.5 mL syringe, SETonic GmbH, Ilmenau, Germany). Conversely, the flow rate of the DMEM was continuously decreased from 125 μL min^{-1} to 0 μL min^{-1} (red channel, Fig. 1C, 2.5 mL syringe, SETonic GmbH, Ilmenau, Germany). This generated a total flow rate of 250 μL min^{-1} for the dispersed phase. Droplets were generated at a flow rate of 500 μL min^{-1} using PFD (blue channels, Fig. 1C, 25 mL syringe, SETonic GmbH, Ilmenau, Germany) with increased droplet spacing realized using a DM. These droplets were guided through the main DM channel (1000 μm diameter). At the same time, the PFD was pumped through an orthogonal side channel (300 μm diameter) at a flow rate of 300 μL min^{-1}. The other side channel was connected to a PFD-filled PTFE tube and closed with a needle.

The flow rate profile was used to generate three droplet sequences. Droplet lengths in the sequences were determined using MedeaLab software (Medea AV Multimedia und Software GmbH, Nuremberg, Germany), and volumes were calculated using a previously published equation.[26] In the first approach, only DMEM was used, flowing through all three channels of the GM. In the second and third approaches, the DMEM in the green channel was displaced with DMSO (D2438, Sigma-Aldrich Chemie GmbH, Taufkirchen, Germany) dissolved in DMEM to a final concentration of 2.82 M and 5.64 M, respectively.

Assessing drug concentration linearity using the continuous flow rate profile

To examine the linear adjustment of the drug concentration in a generated droplet sequence, the introduced flow rate profile was used. In this experiment, DMSO (D2438, Sigma-Aldrich Chemie GmbH, Taufkirchen, Germany) was mixed with resorufin (424455, Sigma-Aldrich Chemie GmbH, Taufkirchen, Germany) to a final concentration of 100 μg mL^{-1}, allowing for measurements within the spectrometer-based AM range. Resorufin is a fluorescent dye and the product of the CellTiter-Blue® cell viability assay. Subsequently, the DMSO was dissolved in the resorufin DMEM mixture to a final concentration of 2.82 M, resulting in a resorufin concentration of 70 μg mL^{-1}. After droplet generation, the droplet sequence was passed through the AM, where the fluorescence intensity was measured at a flow rate of 50 μL min^{-1}. The AM has been designed to enable precise measurement at the emitting wavelength of resorufin. The system comprises a microfluidic AM, a spectrometer (SILVER-Nova, StellarNet Inc., Tampa, FL, USA), and a light source (ILP-2, EVIDENT Germany GmbH, Hamburg, Germany) all connected *via* optical fibres. During the measurement, the droplets were guided through an FEP tube, connected to the microfluidic module of the AM.

Tensiometer measurements using the Wilhelmy-plate method

To determine the surface tensions of DMEM and DMSO (D2438, Sigma-Aldrich Chemie GmbH, Taufkirchen, Germany), the Wilhelmy-plate method was used. Therefore, the bottom edge of a platinum plate was immersed in a bath containing the fluid under investigation, and then placed in a tensiometer (DCAT 25, DataPhysics Instruments GmbH, Filderstadt, Germany). The surface tension was calculated based on the force generated when the plate was pulled out of the fluid (DCATS software, DataPhysics Instruments GmbH, Filderstadt, Germany). Prior to each measurement, the platinum plate was rinsed with deionized water and annealed.

Evaluating the impact of gradient module channels on resorufin mixing

To investigate the influence of the three different channels (red, yellow, and green) on mixing resorufin (424455, Sigma-Aldrich Chemie GmbH, Taufkirchen, Germany) with DMEM, a resorufin solution at 100 μg mL^{-1} was premixed with DMEM and sequentially connected to each channel for the dispersed phase. The remaining two channels were connected to DMEM. The green and red channels (Fig. 3A) were connected to 2.5 mL syringes (SETonic GmbH, Ilmenau, Germany), while the yellow channel (Fig. 3A) was linked to the mixing module (MixM) and the aqueous phase was displaced using a 10 mL syringe (SETonic GmbH, Ilmenau, Germany). All flow rates were controlled *via* a syringe pump (Nemesys, Cetoni GmbH, Korbußen, Germany). The resorufin flow rate was varied between 12.5 μL min^{-1} and 100 μL min^{-1} in 12.5 μL min^{-1} increments. One of the DMEM channels was set to 125 μL min^{-1}, while the flow rate through the other DMEM channel was varied between 112.5 μL min^{-1} and 25 μL min^{-1}. This resulted in resorufin concentrations ranging from 5 μg mL^{-1} to 40 μg mL^{-1} in increments of 5 μg mL^{-1}. The droplets were generated by pumping PFD through the blue channels (Fig. 3A) at a continuous flow rate of 500 μL min^{-1}. The resulting fluorescence intensities for each resorufin concentration were measured using the analysis module (AM).

Comparison of the mixing behaviour of the gradient module with manually premixed resorufin concentrations

To determine the mixing behaviour of the gradient module (GM), a calibration curve was first generated using resorufin in DMEM with final concentrations of 5 μg mL^{-1}, 10 μg mL^{-1}, 20 μg mL^{-1}, and 30 μg mL^{-1}. The solutions were then transferred to the mixing module (MixM) and guided to the yellow channel of the GM with a flow rate of 250 μL min^{-1}. The red and green channels (Fig. 3C) of the GM were

connected to PFD-filled syringes (2.5 mL, SETonic GmbH, Ilmenau, Germany), which were attached to a syringe pump (Nemesys, Cetoni GmbH, Korbußen, Germany) but remained inactive during this experiment. The droplets were generated by pumping PFD through the blue channels (Fig. 3C) at a final flow rate of 500 μL min^{-1}. Following generation, the droplets were stored on an SM, and the fluorescence intensity was measured using the analysis module (AM). Fifty droplets of each sequence were analysed.

To compare the resorufin mixing with the calibration curve, a resorufin solution at 50 μg mL^{-1} was filled into a syringe (2.5 mL, SETonic GmbH, Ilmenau, Germany) and connected to the green channel of the GM (Fig. 3C). The yellow channel was linked to the MixM and filled with DMEM (Fig. 3C). The red channel was connected to a syringe (2.5 mL, SETonic GmbH, Ilmenau, Germany) containing DMEM cell culture medium (Fig. 3C). The droplets were generated with varying flow rates: in the green channel, rates were set at 125 μL min^{-1}, 100 μL min^{-1}, 75 μL min^{-1}, 50 μL min^{-1}, and 25 μL min^{-1}; in the yellow channel, the flow rate was fixed at 125 μL min^{-1}. The red channel was operated at flow rates of 0 μL min^{-1}, 25 μL min^{-1}, 50 μL min^{-1}, 75 μL min^{-1}, and 100 μL min^{-1}. With these settings, concentrations of 5 μg mL^{-1}, 10 μg mL^{-1}, 15 μg mL^{-1}, 20 μg mL^{-1}, and 25 μg mL^{-1} resorufin in DMEM were achieved. The droplets were generated by introducing PFD through the blue channels at a flow rate of 500 μL min^{-1} (Fig. 3C). Comparison of the fluorescence intensity profiles of droplets generated from premixed solutions and those mixed in the GM allowed for assessment of the GM's mixing performance.

Investigation of spheroid proliferation in droplet-based microfluidics

For the spheroid proliferation experiments, a suspension of HEK-293 cells (ACC 305, DSMZ – German Collection of Microorganisms and Cell Cultures GmbH, Braunschweig, Germany) at 6.25×10^5 cells per mL was prepared. The stock solution was diluted to 5×10^5 cells per mL, 3.75×10^5 cells per mL, 2.5×10^5 cells per mL and 1.25×10^5 cells per mL, resulting in approximately 500, 400, 300, 200, and 100 cells per droplet, respectively, for an average droplet volume of 840 nL. The cell suspensions were transferred to the mixing module (MixM) to ensure defined and reproducible cell concentrations within each droplet. Droplets containing the cell suspension were generated using the GM at a flow rate of 150 μl min^{-1} for the cell suspension (yellow channel, Fig. 1C) and 250 μl min^{-1} for the PFD (blue channels, Fig. 1C). The red and green channels (Fig. 1C) were connected to PFD-filled syringes but were not active during the experiment. To prevent droplet merging, the distance between droplets was increased using a DM. This spacing procedure was repeated three times to maintain a flow rate of 200 μl min^{-1} for both the droplet sequence and the PFD.

To verify the amount of seeded cells, droplets were examined directly after generation using an inverse fluorescence microscope (IX81, EVIDENT Germany GmbH, Hamburg, Germany). Spheroid formation and proliferation were monitored daily over a seven-day cultivation period in the droplets (37 °C, 5% CO_2, 80% relative humidity; ICO150, Memmert GmbH, Schwabach, Germany). The increase in the cross-sectional area of the spheroids was analysed for significance using an Ordinary One-Way ANOVA in GraphPad Prism (GraphPad Software Inc., Boston, MA, USA, version 10.2.3). Imaging of the droplets involved performing a scan with 51 images per z-stack across the entire droplet height, which were merged using the extended depth of field imaging (EDF) procedure within the CellSens software (EVIDENT Germany GmbH, Hamburg, Germany). Spheroid proliferation was analysed by determining the cross-sectional area of each spheroid. All images were acquired by connecting the MicM to the microscope.

Calibration of the linear range for cell concentrations in droplets

To generate a dose–response curve, the linear correlation between cell count per droplet and measured fluorescence intensity was determined.

For this experiment, cell suspensions were prepared at stock concentrations of 7.5×10^5 cells per mL and 1.5×10^6 cells per mL. These suspensions were transferred to the mixing module (MixM) and connected to the yellow channel of the GM (Fig. 1C). The cell suspensions were diluted in 10 discrete steps with DMEM cell culture medium, which was connected to the green and red channels of the GM (Fig. 1C). Droplets were generated with a flow rate of 500 μL min^{-1} of PFD (blue channels, Fig. 1C). The cell suspension flow rate was adjusted from 250 μL min^{-1} to 25 μL min^{-1} in 25 μL min^{-1} increments. Accordingly, the flow rate of the DMEM was adjusted from 0 μL min^{-1} to 112.5 μL min^{-1} in 12.5 μL min^{-1} steps for each channel, maintaining a total flow rate of 250 μl min^{-1} for each dilution. These settings yielded cell concentrations ranging from 600 cells to 60 cells per droplet (in increments of 60 cells) and from 1200 cells per droplet to 120 cells per droplet (in increments of 120 cells). Subsequently, the CellTiter-Blue® reagent (Promega GmbH, Walldorf, Germany) was injected into the droplets *via* the CM, with the following parameters: the opening time was set to 5 ms, and the pressure difference was set to 800 mbar. This led to an average injected volume of 200 nL. Following a 4 h incubation at 37 °C, 5% CO_2, and 80% relative humidity (ICO150, Memmert GmbH, Schwabach, Germany), fluorescence intensities were measured using the AM. To determine fluorescence intensities, the SpectraWiz Software (StellarNet Inc., Tampa, FL, USA) was used.

Determination of cytotoxicity of DMSO on HEK-293 cells

This experiment aimed to determine the influence of DMSO (D2438, Sigma-Aldrich Chemie GmbH, Taufkirchen, Germany) on HEK-293 cells (ACC 305, DSMZ – German collection of Microorganisms and Cell Cultures GmbH, Braunschweig, Germany). A cell suspension of 777 500 cells

per mL was mixed in the mixing module (MixM), corresponding to 250 cells per droplet at an average droplet volume of 650 nL. The droplets were generated using the gradient module (GM). The cell suspension was pumped through the yellow channel and mixed with increasing concentrations of DMSO. To achieve the desired DMSO concentrations, DMEM was pumped through the red channel of the GM (2.5 mL, SETonic GmbH, Ilmenau, Germany).

The green channel was connected to a syringe (2.5 mL, SETonic GmbH, Ilmenau, Germany) filled with DMSO in DMEM at a final concentration of 2.82 M. The fluids from the three channels were mixed in a continuous flow rate profile (see Fig. 1D), and droplets were generated with a flow rate of 500 μL min^{-1} PFD (see flow rate profile at Fig. 1D) through the blue channels of the GM (Fig. 1C). To maintain droplet stability and prevent merging, the distances between droplets were first increased by pumping PFD at a rate of 300 μL min^{-1} using a DM next to the GM, then further increased by running the droplet sequence with PFD at 200 μL min^{-1}. All flow rates were controlled using a syringe pump (Nemesys, Cetoni GmbH, Korbußen, Germany). After 20 hours of cultivation, CellTiter-Blue® reagent was injected into each droplet using the CM (parameters: opening time of 5 ms, pressure difference of 800 mbar, injected volume ~200 nL). After an additional four hours of incubation, the fluorescence intensity of the cell mixtures with DMSO was determined using the spectrometer-based analysis module (AM) and the SpectraWiz Software (StellarNet Inc., Tampa,

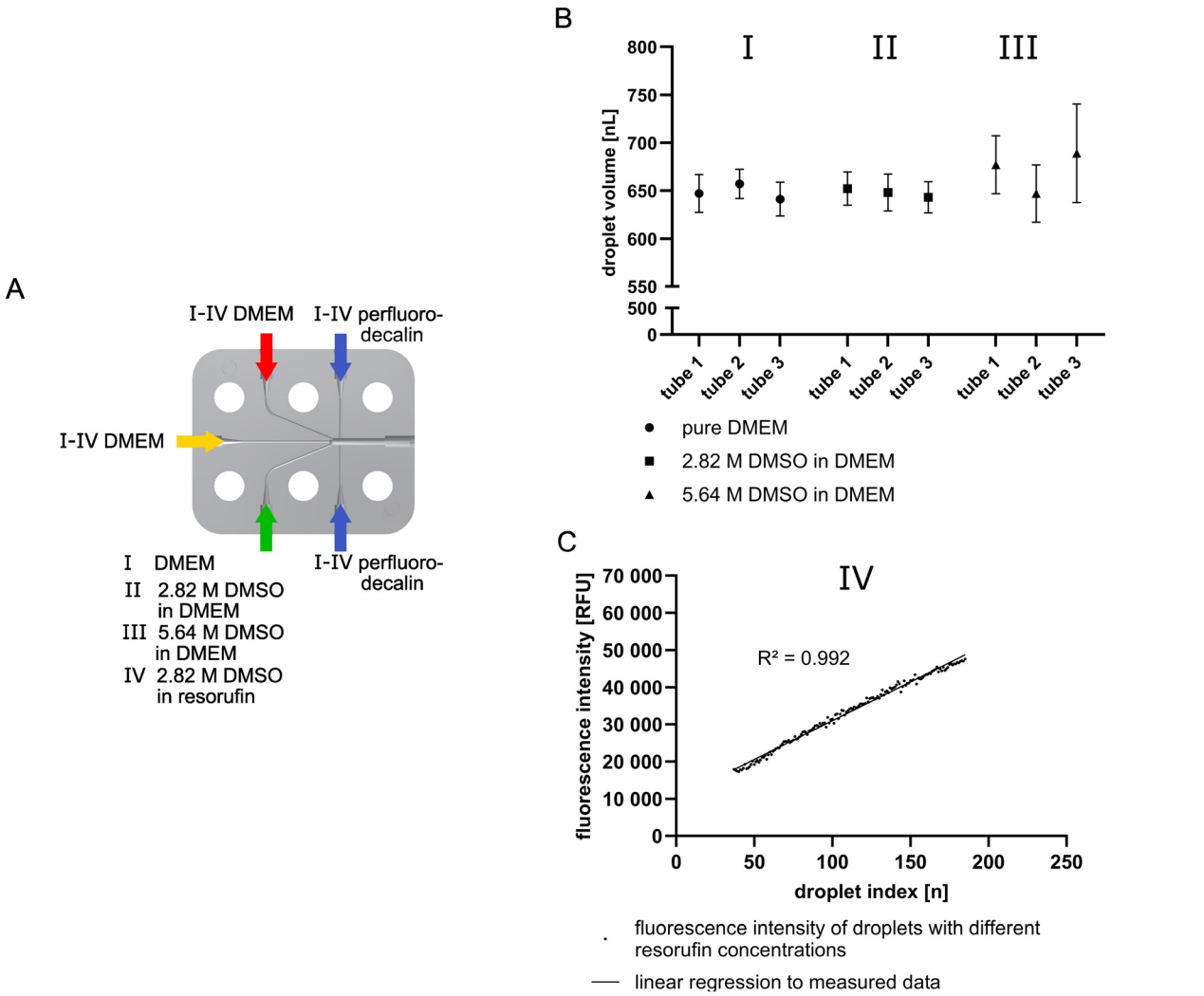

Fig. 2 Characterization of continuous flow rate profiles regarding droplet volume reproducibility in dependence on the drug concentration and injection of varying drug concentrations in terms of linearity in dependence on drug concentration adjustment in resorufin (process step 1, Fig. 1B). (A) Schematic illustration of the GM, detailed dosing of different chemicals per channel, focusing on different aspects: (I) assessment of droplet volume reproducibility when mixing DMEM through the channels for the dispersed phase. (II and III) Evaluation of droplet volume reproducibility when mixing DMEM with DMSO (2.82 M in DMEM (II), 5.64 M in DMEM (III)) through the channels for the dispersed phase. (IV) Mixing of DMEM with resazurin for the characterization of drug concentration adjustments. (B) Mean droplet volume in a single sequence generated with the continuous flow rate profile using the GM for droplet generation. n = 320, mean with SD. (C) Precise adjustment of 148 fluorescence intensities through mixing DMSO (2.82 M) in resorufin (70 μg mL^{-1}) with DMEM (aspect IV). n = 3, mean. The here-tested DMSO concentration range, from 0 M to 1.41 M, corresponds to that used in the later accomplished drug screening experiments.

FL, USA). For the IC_{50} value determination, the first 30 droplets of the sequence, which contained only cell suspension mixed with DMEM but without DMSO, were excluded. A non-linear regression analysis was performed on the data using GraphPad Prism (GraphPad Software Inc., Boston, MA, USA, version 10.2.3) to determine the IC_{50} value.

To compare IC_{50} results obtained with the *pbb* technology to results in a well plate-based setup, the liquid overlay method was used. Two different HEK-293 cell concentrations were exposed to discrete DMSO concentrations (0.14 M, 0.28 M, 0.42 M, 0.71 M, 0.98 M, 1.41 M, 2.82 M, 4.23 M, 5.64 M, 7.05 M, and 8.48 M). First, the wells of a 96-well plate (165305, Thermo Scientific™, Waltham, MA, USA) were coated with 70 μL of agarose (SeaKem® GTG, Lonza, Rockland, ME, USA) at a final concentration of 0.7% [w/v] in PBS. The cell suspension with discrete DMSO concentrations was transferred into the wells. For the comparison of cell numbers per bioreactors (same cell number per droplet and well in different volumes), 250 cells were seeded in 100 μL per well. To compare the cell concentration per mL (different cell numbers per droplet and well), 39 000 cells were seeded in 100 μL per well (250 cells in droplets of 650 nL correspond to ~390 000 cells per mL). After 20 h of incubation, 20 μL of CellTiter-Blue® reagent was added to each well. The fluorescence intensities were measured using a multimode microplate reader (Synergy H1, BioTek Instruments GmbH, Bad Friedrichshall, Germany) after 4 h (higher cell concentration) and 24 h (lower cell concentration) of incubation at an excitation wavelength of 550 nm and an emission wavelength of 590 nm.

3. Results and discussion

Concept of droplet-based cell viability assay

For the establishment of the droplet-based CellTiter-Blue® assay (Fig. 1A), four different process steps (Fig. 1B) were implemented into our modular droplet-based microfluidic *pbb* platform, whose basic setup was introduced previously[26] and is shown in Fig. S1. These steps were realized by specifically designed microfluidic modules. To uniformly generate droplets with defined cell and drug concentrations, a gradient module (GM), which acts as a micro mixer (Fig. 1C), was integrated. A storage module (SM) was used to incubate the cells, both during spheroid formation and incubating the spheroids with different reagents. These reagents were injected into the droplets through a conditioning module (CM). Moreover, to complete the process, a spectrometer-based analysis module (AM) was introduced to analyse the fluorescence based on reagent reduction. For detailed module descriptions, see Fig. S1 and Table S1. This new setup established a standard operating procedure for the droplet-based CellTiter-Blue® assay (see SOP, section 2. Materials and methods). As a central element of this setup, the newly developed GM enabled continuous adjustment of drug concentrations per droplet, with simultaneous uniform cell seeding density (Fig. 1D). This provided the basis for a high-resolution determination of IC_{50} values to validate the drug's efficacy.

The gradient module guarantees highly reproducible droplet generation

To accurately determine IC_{50} values in our droplet-based *pbb* platform, it is essential to ensure the reproducibility of droplet volumes as well as a defined DMSO concentration per droplet. This had to be realized independently of the droplet composition in each generated sequence (process step 1, Fig. 1B). The influence of DMSO itself was tested because it is used as a drug in the final application of this paper (see Fig. 6). To assess this, the DMSO concentrations in the droplets were adjusted using the GM in the continuous flow rate profile with DMEM as the cell culture medium (see Fig. 1D).[27] DMSO was used because, on the one hand, it is a common solvent for drugs, and on the other hand, it is well-known for its influence on the surface tension of liquids. As a control setup, cell culture medium was guided through all three channels as the dispersed phase (Fig. 2A). Subsequently, the cell culture medium in the green channel was replaced with stock solutions of DMSO in DMEM at concentrations of 2.82 M and 5.64 M (Fig. 2A).

Results shown in Fig. 2B indicate that the droplet generation was independent of the DMSO concentration. This allows the use of DMSO concentrations over a broad concentration range from 0 M to 5.64 M. The continuous gradient experiments with the DMEM control and 2.82 M DMSO yielded comparable low standard deviations and an average droplet volume of approximately 650 nL. The microfluidic modules were plasma-functionalized to achieve hydrophobic channel surfaces for successful droplet transport. This indicates that the plasma functionalization used to optimize the channel surface of the modules here was unaffected by the presence of DMSO. This is a significant result, as other workgroups have found that DMSO influences the channel structure during droplet generation, thereby affecting the reproducibility and stability of droplet volumes. For example, Hattori *et al.* introduced a droplet-based microfluidic PDMS chip where the hydrophobic character of the channels decreases over one hour of droplet generation using DMSO, as indicated by the wetting of the channels.[28] In contrast, the plasma functionalization and the material of the chips used here ensured consistent hydrophobization of the channels and a uniform channel diameter for all droplet sequences across different mixtures, as shown in a previous study.[29] This demonstrates that the stability of plasma functionalization is superior to that of PDMS-based microfluidic systems, even using a concentration as high as 5.68 M DMSO, a concentration that exceeds the range relevant to known biological applications.

Assessing the influence of higher DMSO concentrations on droplet volume, generated with 5.64 M DMSO, a slightly larger variation of 6.28% was observed (Fig. 2B, III) compared to the DMEM control (2.90%) (Fig. 2B, I) and

DMSO at 2.82 M (2.78%) (Fig. 2B, II). Moreover, 5.64 M DMSO also showed the strongest influence on droplet volume between individual droplet sequences (Fig. 2B, III). However, the standard deviations observed at 5.68 M DMSO

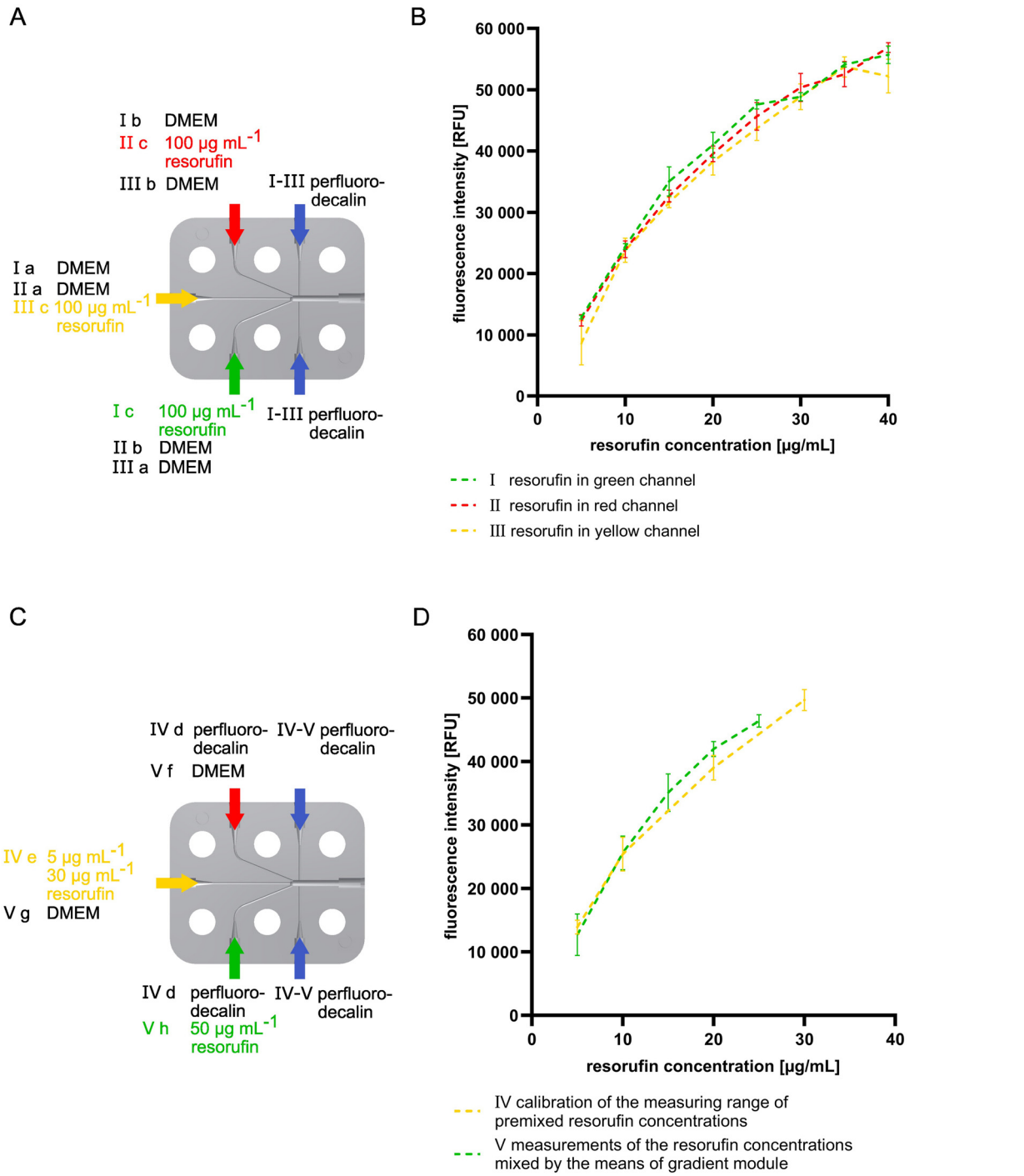

Fig. 3 Accuracy characterization of resorufin concentrations generated during droplet generation using the GM (process step 1, Fig. 1B). (A) Schematic illustration of the connection of the fluids to the GM for the evaluation of the influence of different inlet channels. (B) Accuracy comparison of channels in the gradient module. Resorufin was mixed with DMEM to achieve final concentrations ranging from 5 μg mL^{-1} to 40 μg mL^{-1} in increments of 5 μg mL^{-1}, followed by fluorescence intensity measurements. Resorufin was guided through the green (I), red (II), and yellow (III) channels to determine the influence of each channel. Flow rates were set at 125 μL min^{-1} DMEM (a), 112.5–25 μL min^{-1} DMEM in 12.5 μL min^{-1} steps (b), 12.5–100 μL min^{-1} resorufin in 12.5 μL min^{-1} steps (c). n = 3, mean with SD. (C) Schematic illustration of the connection of the fluids to the GM for the comparison with a conventional pipette. (D) Comparison of resorufin concentrations manually premixed using pipettes (IV) and mixed *via* the GM (V), followed by fluorescence intensity measurements. Flow rates were set at 0 μL min^{-1} PFD (d), 250 μL min^{-1} premixed resorufin (e), 0–100 μL min^{-1} DMEM in 25 μL min^{-1} steps (f), 125 μL min^{-1} DMEM (g), 125–25 μL min^{-1} in 25 μL min^{-1} steps (h). n = 3, mean with SD.

remain below the typical systematic variance of conventionally used pipettes (8%) within the same volume range.

To better understand the impact of DMSO on droplet reproducibility, the surface tensions of DMEM and DMSO were determined using tensiometry. The results demonstrated that DMEM exhibited a surface tension of 54.39 mN m^{-1}, while DMSO had a lower value of 44.35 mN m^{-1}. These results are consistent with findings from Nastasa *et al.*, who showed that surface tension decreases with increasing DMSO concentrations in water using the pendant droplet method.[30] Therefore, the different surface tensions between DMEM and DMSO, and not the limits of the *pbb* technology, are responsible for the higher standard deviations in droplet volumes. Overall, with the *pbb* technology, droplets were successfully generated over a long-term period within biologically relevant DMSO concentration ranges without adversely affecting the GM material. Based on these results, a concentration of 2.82 M DMSO was selected for later drug screening applications (see Fig. 6). Using the continuous flow rate profile, a maximum final concentration of 1.41 M in the droplets can be realized (see Fig. 1D). Notably, these DMSO concentrations are comparable to those typically used for cryo-conservation.

High-resolution adjustment of 148 different drug concentrations in one droplet sequence

To further validate the system's precision, the linearity of drug concentration adjustment within a single droplet sequence was systematically analysed (process step 1, Fig. 1B). For this, DMEM cell culture medium (yellow and red channels, Fig. 2A) was mixed with resorufin that had been pre-diluted in DMSO, and fluorescence intensities were measured using the AM. The resulting data demonstrated a strong linear correlation between fluorescence intensity and increasing resorufin concentrations, with a regression coefficient of R^2 = 0.992 from 17 000 to 47 000 relative fluorescent units (RFU) (Fig. 2C). The minimal variation between regression slopes (200.5, 209.2, 209.4) across different experiments (averaged in Fig. 2C) demonstrated that the system reliably enabled comparable drug concentration profiles across different experiments. This approach successfully realized up to 148 different DMSO concentrations per droplet sequence with reproducible cell concentrations. Fig. 2C illustrates the resulting linear increase in fluorescence intensity across the droplet sequence.

In comparison to other methods, this approach provides high-resolution concentration adjustments. In literature, other channel geometries have been described for generating a smaller number of concentrations. Rho *et al.* developed a mixer that achieves linear concentration adjustments using rhodamine, where 35 droplets were analysed, yielding a regression coefficient of R^2 = 0.999.[31] Chen *et al.* developed a coaxial tube system for forming metal–organic frameworks, which enabled the achievement of 12 different concentration steps.[32] Additionally, Chen *et al.* developed a well plate-like microfluidic array for drug screening approaches, using a specialized sliding technique and a PDMS chip.[33] This system allows for variation across different drug concentrations, with a maximum range of 0 mM to 0.7 mM. Compared to those approaches, the *pbb* technology allows for both a higher number of concentrations and a broader concentration range to be investigated.

A comparison of all these systems highlights the *pbb* technology as the one with the highest resolution for drug concentration adjustment, enabling up to 148 steps. Consequently, the technology, combined with the continuous flow rate profile, is well-suited for linear drug concentration gradients within a single droplet sequence. To our knowledge, the *pbb* technology currently outperforms other microfluidic and well plate-based approaches in both resolution and flexibility.

Highly accurate mixing across all inlet channels of the gradient module

In droplet-based microfluidics, different strategies are employed to mix various fluids, including co-flow, fluid injection, and mixing due to the channel structure.[34] In this study, the GM utilized structural mixing, where the three aqueous streams converged just upstream of the droplet generation area, effectively ensuring consistent and stable concentrations without concentration variability. To evaluate the influence of channel selection on resorufin concentration within the dispersed phase, a dilution series was prepared with resorufin, connected to each of the three channels (red, yellow, and green), and diluted using DMEM through the remaining two channels (see Fig. 3A).

The fluorescence intensities for the green channel ranged from 12 843 RFU to 55 683 RFU. For the yellow channel, intensities ranged from 8672 to 52 242 RFU, while for the red channel, intensities between 12 324 RFU and 56 877 RFU were measured. The data demonstrates a consistent trend across all channels, affirming that the channel selection does not impact the resulting resorufin concentration. A wide range of resorufin concentrations was successfully quantified spectroscopically, with comparable mixing efficiency observed in each data point. The highest deviations between the green and yellow channels were observed at concentrations of 15 μg mL^{-1}, 20 μg mL^{-1}, and 25 μg mL^{-1}. However, overlapping standard deviations indicate that these differences are statistically not significant. At concentrations above 25 μg mL^{-1}, fluorescence intensities deviate from linearity, which is due to well-documented saturation effects associated with resorufin fluorescence measurements. Here, signal saturation was observed at fluorescence intensities exceeding 40 000 RFU. Consequently, there is no limitation for the AM (see Fig. S1D). Furthermore, this effect only appears beyond the relevant fluorescence units for all tested cell concentrations (see Fig. 5) and for the drug screening approach (Fig. 6).

Overall, the GM proves to be a high-precision mixing module, regardless of the selected channel. It enables reliable results across the entire fluorescence range relevant to cell viability assays (Fig. 5 and 6).

The gradient module replaces the pipette in the laboratory for time-efficient mixing of fluids to defined concentrations

The GM offers significant time-saving advantages by automating the mixing of solutions, thereby reducing the need for manual pipetting. To further characterize the GM's mixing performance, fluorescence intensities of manually premixed solutions were compared to those produced by the GM. Fig. 3C provides a schematic illustration of the GM with the connected fluids for each dilution, along with corresponding fluorescence intensities, measured using the AM, are shown in Fig. 3D.

The measured fluorescence intensities of the manually premixed solutions ranged from 13 892 RFU (5 μg mL^{-1}) to 49 647 RFU (30 μg mL^{-1}), while GM-mixed concentrations produced intensities between 12 704 RFU (5 μg mL^{-1}) and 46 378 RFU (25 μg mL^{-1}). No significant differences were observed between the premixed and GM-mixed samples, as indicated by the comparable standard deviations, suggesting similar reproducibility. Unlike pipetting robots, the *pbb* technology offers the advantage of automated, time-efficient, discrete adjustment of defined resorufin concentrations by adapting the flow rate. As a pipette-based alternative, Mao *et al.* developed a nano pipette using standard pipette tips. This system, comparable to pipetting robots, was evaluated for its injection precision against other commonly used pipettes.[35] The findings of Mao *et al.* show superior performance of the nanopipette compared to commonly used pipettes. While the nanopipette excels in precision, the *pbb* platform offers a higher degree of automation and is especially advantageous in terms of scalability and its all-in-one capabilities.

Furthermore, with its compact dimensions of only 52 × 40 × 30 cm, the *pbb* system offers a space-efficient solution ideally suited for high-throughput applications, especially in small laboratories. Beyond scalability and automation, the *pbb* technology also supports a variety of analytical readouts. In droplet-based microfluidics, various optical detection methods are available for measuring enzyme kinetics, including epifluorescence imaging, absorbance, and fluorescence measurements.[34] Accordingly, the data obtained using premixed resorufin concentrations were also used to evaluate the sensitivity of the AM. The measured fluorescence intensities correspond to the range of resorufin that can be produced by viable cells through the reduction of resazurin in the CellTiter-Blue® assay (process step 3, Fig. 1B). A linear correlation was observed between the measured fluorescence intensities and the resorufin concentrations over the range of 5 μg mL^{-1} to 20 μg mL^{-1} (Fig. 3D). These values are comparable to those obtained from resorufin mixed with DMSO (Fig. 2C), which serve as the basis for determining the IC_{50} of DMSO in the viability assay (Fig. 6).

Notably, the *pbb* technology enabled the precise mixing of DMEM with resorufin, while simultaneously incorporating predefined DMSO concentrations used in the final drug screening setup, demonstrating the system's practical applicability. As a result, about 10 pipetting steps were saved in the results discussed here. In the case of drug screening using the continuous flow rate profile with up to 290 concentrations, hundreds of pipetting steps are saved by using the GM (see Fig. 6). Consequently, the GM offers significantly improved efficiency compared to manual pipetting, due to its automated mixing strategy.

pbb – an important technology for 3D disease modelling

Based on the optimized mixing and droplet generation methods established in the previous section, next, the influence of cell seeding density on HEK-293 spheroid formation and proliferation within droplets was analysed. In recent years, 3D cell culture has increasingly become the standard for precise IC_{50} determination in drug screening applications, as 3D cell structures (*e.g.*, spheroids) are recognized as highly accurate *in vitro* models, providing valuable insights into cell–cell and cell–ECM interactions.[36]

Different techniques for forming spheroids are available and can be broadly categorized into scaffold-based and scaffold-free approaches. In scaffold-based systems, cells adhere to or are encapsulated in ECM-like matrices that promote 3D aggregation and support structural stability, thereby forming *in vivo*-like models.[37] This includes hydrogels such as alginate or Matrigel®, which are often used in both well plates and droplet-based microfluidics.[38,39]

Scaffold-free techniques rely on the self-assembly of cells in suspension. Common examples in well plates include the "hanging droplet" and "liquid overlay" methods, which are supported by low attachment well plates or agarose coating to prevent cell adhesion to the plate surface.[40–42]

The *pbb* technology also follows a scaffold-free approach. Spheroids are formed through spontaneous self-assembly within droplets, without the use of additional matrices or support structures. This strategy is conceptually similar to the liquid overlay technique, but implemented in a continuous, microfluidic environment that enables enhanced control and integration into automated workflows.

In droplet-based microfluidics, precise droplet volume and homogenous cell distribution are essential to ensure reproducible spheroid formation. Singh *et al.* have demonstrated that the diameter of spheroids in well plates varies significantly with seeding density and volume, ranging from 400 μm to 700 μm at seeding densities of 4000 to 8000 cells per well.[43]

The *pbb* platform addresses this challenge through reliable droplet generation and consistent cell loading, enabled by the integrated mixing module (MixM; see Fig. S1A). Furthermore, Lemke *et al.* described a more uniform formation of embryoid bodies of murine embryonic stem cells compared to the well plate-based technology by using *pbb*.[7]

To establish an optimal model for subsequent drug screening experiments, different initial seeding densities of HEK-293 cells were evaluated for consistent spheroid formation and sustained proliferation in the *pbb* platform.

Fig. 4 illustrates the progression of spheroid cross-sectional areas from day 2 to day 7 of cultivation for different HEK-293 cell seeding densities per droplet (process step 2, Fig. 1B). Spheroids seeded with 200 and 300 cells per droplet supported spheroid proliferation up to day six in all experiments. Notably, the spheroids seeded with 200 cells demonstrated the best proliferation as analysed by spheroid cross-sectional area, with an increase from 22 134 μm^2 (day 2) to 35 601 μm^2 (day 6). This increase was statistically significant from day 2 to day 5, as confirmed by ordinary one-way ANOVA. Similarly, spheroids seeded with 300 cells increased from 26 074 μm^2 to 36 000 μm^2 over the same period; however, this trend was not statistically significant. These results are consistent with the general understanding that each cell line has an optimal cell seeding density for 3D cell cultures in well plates. A similar dependency has already been reported for the *pbb* technology.[7] Based on the current data, a seeding density of about 200 cells per droplet appears optimal for supporting sustained HEK-293 spheroid proliferation within the *pbb* environment (Fig. 4A). Overall, the consistent data and the reproducible spheroid formation in the droplets demonstrate that the *pbb* technology provides an excellent foundation for 3D cell culture, offering great promise for advanced 3D disease modelling.

The droplet-based microfluidic platform introduced here supports the proliferation of HEK-293 spheroids in small volumes of approximately 800 nL. It is widely acknowledged that the ratio between medium volume, medium composition, and cell number critically influences cell proliferation, primarily due to the availability of nutrients.[44] Yoshimura *et al.* demonstrated that increasing the culture medium volume from 0.4 mL to 2.0 mL per well in a 24-well plate resulted in a reduction in the total number of osteoclasts, while promoting the formation of larger osteoclasts with 8 or more nuclei.[45] This underlines the importance of balancing medium volume and cell number in 3D cell cultures. Despite the small droplet volume, the *pbb* technology ensures sufficient nutrient supply for the validated initial cell number, enabling robust spheroid formation and contributing to resource efficiency through reduced reagent consumption. To facilitate cell proliferation in principle, droplets exceeding 1 mm in length are generated, specifically tailored to cell-based approaches. These droplets were substantially larger than those presented by Weigel *et al.* (58 μm to 443 μm), who did not cultivate cells in the droplets.[46]

To realize spheroids with diameters exceeding 300 μm, higher seeding densities of 400 and 500 cells per droplet were evaluated. These cell numbers correlate to 50 000 and 62 500 cells per well in a standard 96-well plate format. Despite stable spheroid formation, higher seeding densities resulted in reduced proliferation rates, as determined by the consistent spheroid cross-sectional area over 7 days of cultivation (Fig. 4B). This finding is consistent with those of Jones *et al.*, who reported earlier proliferation arrests in rat basophilic leukaemia cells in well plates.[47] Proliferation was arrested on day 4, with initial cell counts ranging from 2000 to 5000 cells per well.

In contrast, 500 to 1000 cells per well continued to proliferate up to day 9. Accordingly, the *pbb* technology mirrors established trends observed in well plates, where lower seeding densities promote extended proliferation. Notably, spheroid formation occurred *via* self-assembly in a broad range of seeded cell densities, without the need for additional hydrogel or other ECM-mimicking components within the *pbb* technology. This is facilitated by the hydrophobic nature of PTFE tubing and PFD, which prevents cell adhesion to surfaces.

The *pbb* technology enables the generation of highly reproducible single spheroids in ultralow amounts of cell culture medium (Fig. 4A), supporting both sustainability and scalability. Based on these findings, a cell seeding density of 250 HEK-293 cells per droplet was selected for the drug screening experiments, as it reliably produced spheroids of suitable size and biological relevance.

Calibration of cell density ranges for accurate IC_{50} determination using CellTiter-Blue® assay

Following the evaluation of HEK-293 spheroid proliferation based on the seeded cell density, the next step focused on calibrating the linear range of CellTiter-Blue® fluorescence intensity and viable cell number to ensure precise IC_{50} determinations during drug screening. The CellTiter-Blue® assay is based on the principle that only viable cells can reduce resazurin to the fluorescent resorufin. As a result, fluorescence intensity directly correlates to cell viability, enabling reliable quantification of viable cells per droplet. To ensure precise data interpretation, it was therefore essential to calibrate the range over which this correlation remains linear.[48]

For calibration, CellTiter-Blue® fluorescence intensities were determined at defined concentrations of HEK-293 cells, generated using the discrete flow rate profile and subsequently measured with the spectrometer-based AM.

As shown in Fig. 5, fluorescence intensities were successfully detected corresponding to cell concentrations ranging from 120 to 1200 cells per droplet (process step 3, Fig. 1B). The linear range was investigated in two segments: 120 to 600 cells per droplet and 240 to 1200 cells per droplet (Fig. 5C). The successful adaptation and influence of the cell concentration per droplet are presented in Fig. 5D–I.

Using the discrete flow rate profile, two initial cell stock solutions (7.5×10^5 cells per mL and 1.5×10^6 cells per mL) were diluted into ten defined cell concentrations (Fig. 5A). The calibration data revealed two linear graphs with slightly different slopes, confirming that both lower and higher cell concentrations per droplet can be precisely calibrated using

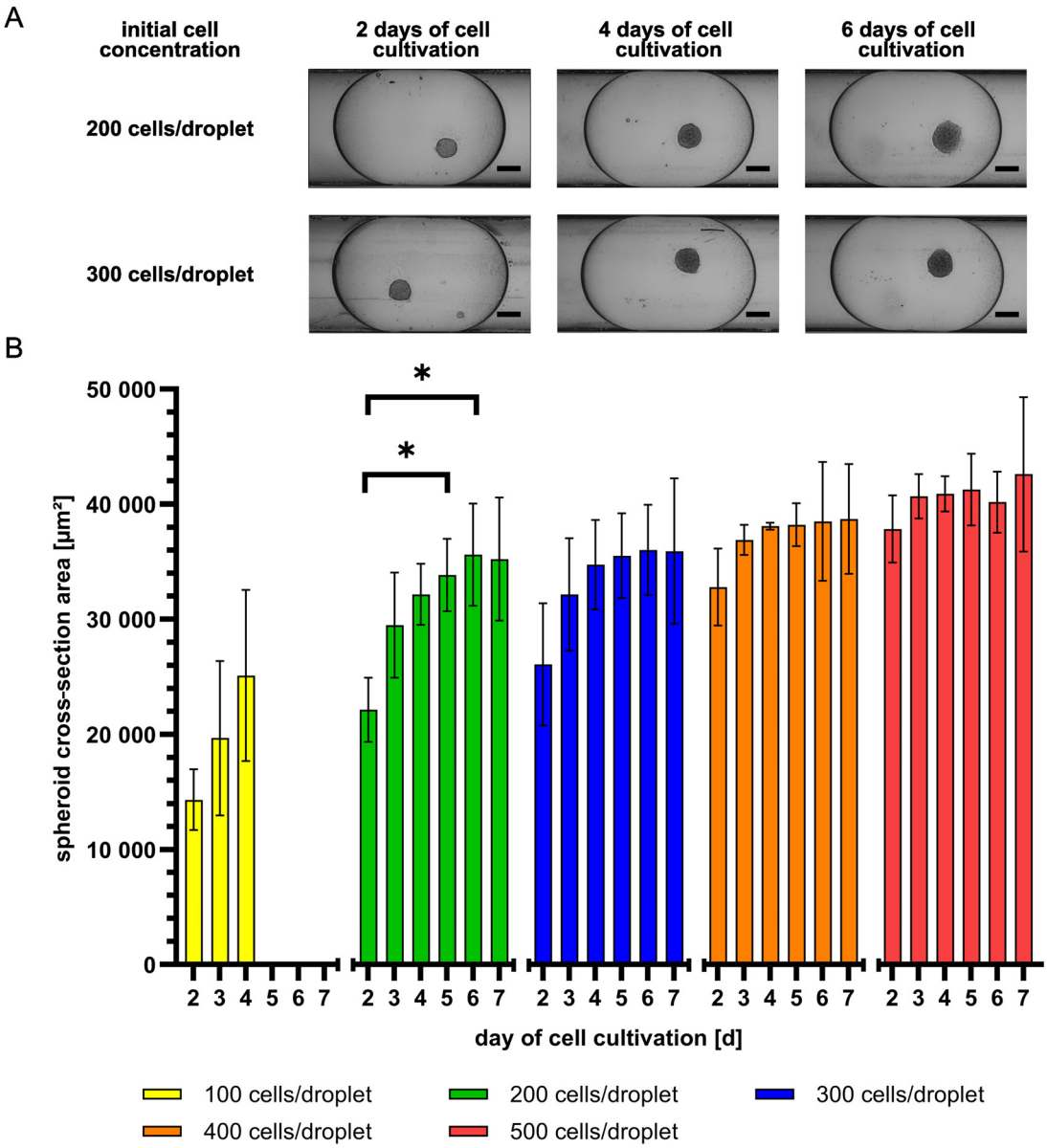

Fig. 4 Influence of cell seeding density on formation and proliferation of HEK-293 spheroids. Spheroids were analysed over 7 days of cultivation in droplet-based microfluidics (process step 2, Fig. 1B). (A) Representative extended depth of field (EDF) images from spheroids cultured in droplets with a seeded cell count of 200 ( ) and 300 ( ) cells per droplet. Images were recorded after 2, 4, and 6 days of cultivation. Scale bar: 200 µm. (B) Influence of cell seeding density on HEK-293 spheroid formation and proliferation in droplets. The cell seeding density ranged from 100 to 500 cells per droplet. Spheroid proliferation was analysed using the spheroid cross-sectional area. n = 3, mean with SD, *$p > 0.05$.

the *pbb* technology. Although minor deviations were observed, likely due to slight local variations in the initial cell stock concentration outside of the *pbb* system, both data sets presented strong linearity between cell concentration and fluorescence intensity (Fig. 5C). In comparison, the linear range of CellTiter-Blue® in the traditional 96-well plate format extends to approximately 50 000 cells per well, which roughly corresponds to 400 cells per droplet in the *pbb* technology. Remarkably, these findings demonstrate that the *pbb* platform allows quantification of higher cell concentrations per mL than is typically achievable in well plates.[49] Furthermore, because the droplet sequence resulting from the discrete flow rate profile, including all defined cell concentrations, is enabled in about 5 minutes, the system operates highly efficiently in terms of time.

In terms of sensitive analyses, fluorescence-based detection is one of the most used strategies in droplet-based microfluidics. Other commonly used techniques include fluorescence imaging and laser-induced fluorescence measurements.[50] For example, An *et al.* used fluorescence microscopy to detect varying concentrations of *Salmonella* in droplets.[51] At the same time, Uzarski *et al.* demonstrated a linear relationship between fluorescence intensity and cell concentration in the range of 0.05×10^6 to 1×10^6 cells per mL,

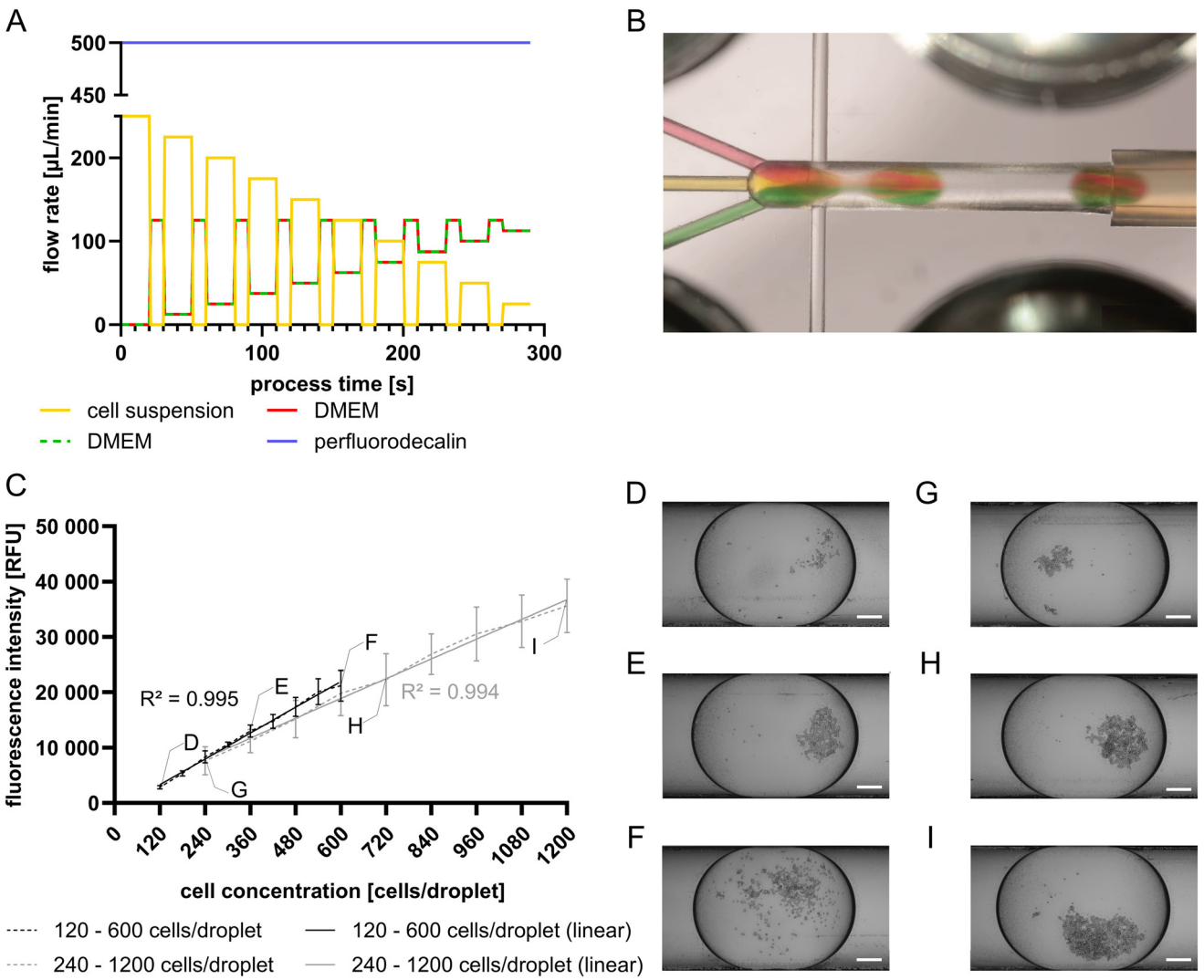

Fig. 5 Determination of the linear range of cell concentrations in droplets using the viability assay. (A) A flow rate profile for seeding 10 discrete, defined cell concentrations is generated within a single droplet sequence in five minutes. The flow rates of the cell suspension and DMEM resulted in a reproducible flow rate of 250 µL min^{-1}. (B) Photograph of the GM mixing differently coloured dyes, resulting in dispersed phases. (C) Illustration of the linear range of the measured fluorescence intensities of droplets using the AM (process step 4, Fig. 1B) for discrete steps of different seeded cell counts (process step 1, Fig. 1B) after 4 h of incubation with the assay reagent (process step 3, Fig. 1B). The black graph shows measurements of droplets containing 120 to 600 cells, while the grey graph illustrates measurements of droplets containing 240 to 1200 cells. n = 3, mean with SD. (D–F) Representative images of droplets (associated with the black graph) from process step 1 containing (D) 120 cells, (E) 360 cells, (F) 600 cells, (G–I) Representative images of droplets (associated with the grey graph) from process step 1 containing (G) 240 cells, (H) 720 cells, (I) 1200 cells. Scale bar: 200 µm.

using epithelial cells and fibroblasts in a perfusion cultivation chamber.[52] Similarly, Lim *et al.* found a linear relationship between *Trypanosoma brucei rhodesiense* concentration and fluorescence intensity after 8 hours of resazurin incubation, spanning a range of 1 × 10^6 to 3 × 10^6 unicellular organisms per mL.[53] In the past, bacterial growth has been successfully demonstrated in *pbb* with cell densities comparable to those in conventional shake flask cultures.[54] Although the CellTiter-Blue® assay has not been specifically applied in this context, its transferability has been demonstrated elsewhere, making a successful implementation within *pbb* highly plausible.

The calibration data, covering a range of 120 to 1200 cells per droplet, fully encompass the proliferative range of HEK-293 spheroids used in drug screening (Fig. 6), thereby confirming the applicability of the *pbb* platform for precise, fluorescence-based viability analysis.

Overall, the *pbb* technology presented here offers the unique ability to calibrate a linear range of fluorescence intensities from viable cells across a wide concentration range within five minutes. This represents a significant time advantage over well plate-based technology. Each droplet is individually distinguishable, allowing for temporal monitoring of droplet contents for comparative evaluation.

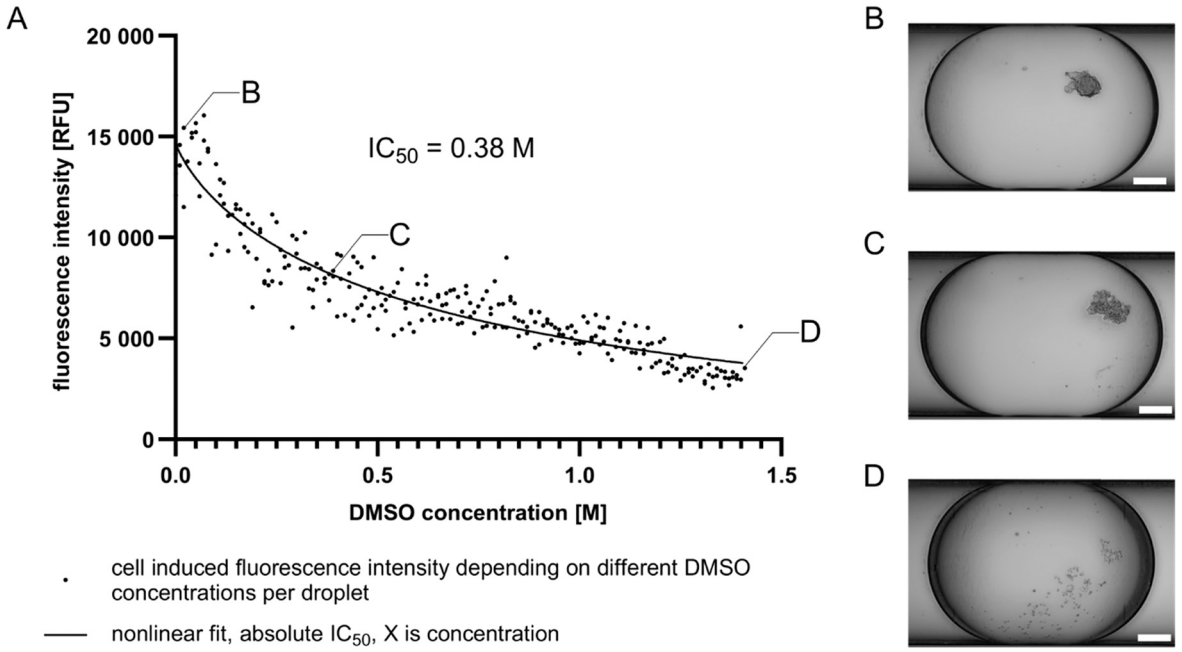

Fig. 6 Dose–response curve and IC_{50} analysis of DMSO for HEK-293 cells. (A) Dose–response curve for 290 continuously adjusted concentrations using the GM (process step 1, Fig. 1B). Viability assay reagent was injected 20 h after cell seeding using the CM (process step 3, Fig. 1B). Fluorescence intensities were determined with the spectrometer-based AM (process step 4, Fig. 1B) 4 h after reagent injection. (B) A droplet containing a spheroid cultivated with pure cell culture medium. (C) Droplet containing a cell cluster, which has not formed a spheroid, exemplarily for the IC_{50} DMSO concentration at 0.38 M. (D) Droplet containing single cells at the highest DMSO concentration of 1.41 M. n = 3, mean. Scale bar: 200 μm.

The established standard curve covers quantification of higher cell concentrations per mL than well plate-based systems and serves as a robust basis for the validation of IC_{50} determination in HEK-293 cells treated with DMSO. The resulting fluorescence intensity (Fig. 5C) exhibits a linear correlation comparable to that of the calibration curve shown in Fig. 2C.

pbb enables IC_{50} values with higher resolution compared to the state of the art

Building upon the established calibration of fluorescence intensity and viable cell concentration, the modular microfluidic *pbb* platform was used to determine the viability of HEK-293 cells exposed to DMSO. DMSO, commonly used as a solvent in cancer therapies but cytotoxic at higher concentrations, serves as the model drug for determining the IC_{50} in this study. Here, we used the continuous flow rate profile to generate 290 DMSO concentrations. For the drug screening, 250 HEK-293 cells per droplet were automatically seeded. The cells were initially exposed to DMSO during the droplet generation process to ensure a standardized incubation of exactly 24 h for each droplet. Consequently, a higher number of concentrations was investigated compared to the calibration of the fluorescence intensities (see Fig. 2C).

As shown in Fig. 6A (process step 4, Fig. 1B), the fast dose–response analysis revealed an IC_{50} value of 0.38 M DMSO for HEK-293 spheroids. This DMSO concentration can be considered a crucial reference for drug screenings. In most cancer cell-based assays, this concentration is not exceeded, as DMSO is primarily used as a solvent for drugs. In some cases, however, the critical drug concentration of chemotherapeutic agents is close to their solubility limit, so that the solvent's own influence must be considered for the dose–response results.

In this context, it is worth noting that cells are cryopreserved with up to 1.41 M DMSO in FCS, the maximum concentration achievable with 2.82 M in this setup. The investigated concentration range, therefore, spanned from 0 M to 1.41 M in droplets. The continuous flow rate profile allows for increments of 0.34% of the drug stock solution used. Results also indicate that the lowest DMSO concentration already impacts HEK-293 cell viability, and no upper plateau of concentration dependence was identified. Taken together with the determined IC_{50} of only 0.38 M, it is paramount that cryopreserved cells are treated with utmost care and speed to prevent any damage to the cells.

To ensure that the observed cell viability was solely attributed to DMSO and not influenced by leakage or diffusion of substances into the PFD, the chemical stability of the fluidic environment was evaluated. Previous work by Waeterschoot *et al.* discussed the suitability of perfluorinated oils, such as the PFD used in this study, for droplet-based applications.[55] Due to their low hydrogen-bonding capacity and weak London dispersion forces, polar and non-polar chemicals do not leak to the continuous oil phase when

using pure PFD, an issue that has been previously described for systems using surfactant-stabilized oils.[55,56] In line with this, no visible coloration of the PFD phase and a stable fluorescence baseline were observed throughout all experiments, indicating that neither resazurin nor DMSO significantly diffused out of the aqueous phase. This chemical stability, combined with the rapid and precise determination of the IC_{50} value, emphasizes the outstanding suitability of the *pbb* technology in drug screening approaches.

Fig. 6B–D visualizes the morphological impact of increasing DMSO concentration on spheroid formation. In droplets without DMSO, spheroid formation occurred within 24 hours after seeding. However, at 1.41 M, DMSO spheroid formation was completely inhibited and droplets only contained single cells. At a DMSO concentration of 0.38 M, only cell clusters remained, indicating an incomplete spheroid formation mirroring the IC_{50} derived from fluorescence measurements (see Fig. S2 for further representative images at different DMSO concentrations). This morphological effect further validates the viability-based quantification and highlights the system's sensitivity to subtle differences in drug concentration.

To benchmark the IC_{50} values obtained with the *pbb* technology, reference measurements were carried out using a standard 96-well plate format with a 100 μL volume per well. As this represents a 150-fold difference in volume compared to a droplet, two seeding densities were tested: 250 cells per well, equivalent to the cell number per bioreactor (*i.e.*, well and droplet), and 39 000 cells per well, matching the cell concentration per mL. The resulting IC_{50} values for DMSO were 0.84 M (250 cells per well) and 4.68 M (39 000 cells per well), representing a 5-fold difference between the two (see Fig. S3 and S4), indicating that cell concentrations significantly influence drug sensitivity. Notably, the IC_{50} of the lower cell concentration (250 cells per well) is closer to the IC_{50} value in droplet-based microfluidics (0.38 M). The reason for the slightly higher IC_{50} value in the well plates compared to *pbb* could be the difference in relative culture volume. If cell metabolism is comparable in both systems, the gradient of metabolic production, as well as nutrient depletion, is higher in a lower cultivation volume. Comparing both well plate-based screenings, the higher IC_{50} value at 39 000 cells may be attributed to the greater number of cells in the wells. As the cells settle in the wells and form several cell layers, they can protect each other from the influence of the DMSO, as diffusion through these layers is impeded. When comparing different volumes with the same cell concentration, the cells may be more stressed due to the lower volume in the droplets, resulting in lower IC_{50} values compared to the 96-well plate. This could be a consequence of the well-known effect of the volume of cell culture medium on cell proliferation.[57]

Previous studies, such as those by Prince *et al.*, presented microfluidic arrays developed to determine IC_{50} values in breast cancer organoids for a personalized medicine approach, where the samples were arranged in well plate-like chambers and only discrete drug concentrations were tested.[58] In contrast, the *pbb* technology offers a continuously adjustable, high-resolution dilution strategy, unlike traditional well plate-based systems, where drugs are only tested in fixed concentration steps.[59,60] To our knowledge, the *pbb* technology presents the first system that allows a continuous linear adaptation of drug concentrations for high-resolution IC_{50} determination.

Compared to other microfluidic systems, such as the platform by Tomasi *et al.*, which uses RGB values and a CCD camera to evaluate the viability of stained spheroids,[61] the *pbb* technology offers faster and more efficient IC_{50} analysis by using spectrometer-based AM to determine fluorescence intensities.[26] Using the system of Tomasi *et al.*, fluorescent images must be evaluated. The spectrometer-based AM, in contrast, enables the determination of droplet fluorescence intensities under flow conditions enables the analysis of up to 290 droplets in 40 minutes, significantly reducing analysis time and complexity. Overall, high-resolution IC_{50} value determination across 290 distinct concentrations was achieved within a single droplet sequence, a capability that, to our knowledge, is unique to the *pbb* technology to date.

Building on its modular character, the flexibility of the GM, and the sequential arrangement of the droplets within the tubes, the *pbb* platform enables a time-saving analysis of IC_{50} values compared to other droplet-based systems. With these advantages, the droplet-based microfluidic *pbb* platform is clearly distinguished from current state-of-the-art systems. Here, the influence of DMSO on spheroid formation and the viability of HEK-293 cells was examined. It is well-known that the effects of drugs differ when applied to already formed spheroids, due to cell–cell and cell–matrix interactions in 3D cell culture models that influence drug penetration and sensitivity. Since the focus here was the linear adjustment of the drug concentration, DMSO was initially mixed with HEK-293 single cells during droplet generation. As the CM also allows the precise injection of drugs at a volume between 19 and 435 nL in 40 nL steps, a drug screening with already formed spheroids with discrete drug concentrations is also possible within the *pbb* technology, thus expanding the system's versatility for more complex drug testing scenarios in the future.[26]

4. Conclusion

The highly flexible droplet-based *pbb* technology enabled the precise adjustment of a continuous flow rate profile, allowing for the reproducible generation of droplets with defined cell concentrations and linearly increasing drug concentrations. This enabled the creation of 290 distinct conditions within a single droplet sequence, allowing for the high-precision determination of the IC_{50} of DMSO in HEK-293 cells. A comprehensive characterization of the newly developed gradient module (GM) revealed a mixing process that offers

advantages over manual pipetting, highlighting its potential to replace pipettes in future laboratory workflows. Moreover, the microfluidic modules manufactured in-house were shown to exhibit channel-independent mixing behaviour, and their plasma functionalization remained stable over a broad range of DMSO concentrations (1.41 to 5.64 M) for at least eight hours.

The platform also proved highly suitable for 3D cell culture. These 3D models are generated without the use of hydrogels through a self-assembly process. This, along with the highly reproducible proliferation of HEK-293 cells to form spheroids in droplets, demonstrates the high potential and importance of the droplet-based microfluidic platform for 3D disease modelling. Additionally, generating droplets without surfactants eliminates any potential impact on spheroid formation and proliferation. This droplet-based setup overcomes the limitations of conventional 2D monolayers by enabling physiologically highly relevant cell–cell and cell–matrix interactions. Moreover, the microenvironment within the *pbb* platform can be tailored using the GM and the conditioning module (CM) to meet the specific needs of different cell types.

To reliably determine IC_{50} values using the CellTiter-Blue® assay, the linear range of fluorescence intensity across cell concentrations (120 to 1200 cells per droplet) was established using the analysis module (AM). Combined with the continuous flow rate profile, this facilitated linear adaptation of the DMSO concentrations, resulting in a time-efficient and high-resolution determination of the IC_{50} for HEK-293 spheroids. An IC_{50} value of 0.38 M DMSO was determined by adapting 290 different drug concentrations at a seeding cell density of 250 cells per droplet. The fast determination of high-resolution IC_{50} values demonstrates a significant advancement over current drug screening methods. All essential process steps for a standardized cell viability assay were successfully implemented with high precision within the *pbb* workflow, highlighting its potential for broader applications. Due to the modular design, further workflows and processes can be added with minimal adaptation.

Building on these findings, future studies will expand the use of the CellTiter-Blue® assay to different cancer types and drug candidates, aiming to support personalized medicine approaches. Patient samples and primary cells will be integrated into the droplet-based microfluidic platform for individualized IC_{50} profiling. Independent of the size of primary tumors, the *pbb* platform requires fewer chemicals and primary tumor cells to determine the IC_{50} value, thereby facilitating the development of patient-individualized therapies. This underlines the sustainable character of the *pbb* technology. Furthermore, undifferentiated Acta 2 murine embryonic stem cells have already been used within this technology, and ongoing investigations are exploring their use in disease modelling (not shown here).[7] In addition, the successful cultivation of bacteria within the *pbb* technology[54] lays the foundation for future studies in infection biology, where the completely closed character of the *pbb* platform is an advantage. Given its adaptability and capacity to create tailored microenvironments, the platform holds strong potential for the development of advanced disease models.

Abbreviations

3D	Three-dimensional
pbb	*Pipe based bioreactors*
SOP	Standard operating procedure
FCS	Fetal calf serum
GM	Gradient module
DMSO	Dimethyl sulfoxide
MixM	Mixing module
DM	Droplet module
CM	Conditioning module
AM	Analysis module
SM	Storage module
MicM	Microscopy module
PFD	Perfluorodecalin
EDF	Extended depth of field
RFU	Relative fluorescent units

Author contributions

Conceptualization, S. W., K. L., and J. M. K.; methodology, M. S., J. M. K., and F. M.; software, S. W.; validation, M. S.; formal analysis, M. S. and F. M.; investigation, M. S.; resources, K. L. and S. W.; data curation, M. S. and S. W.; writing, original draft preparation, M. S.; writing, review and editing, K. L., F. M., and D. H.; visualization, M. S., K. L., F. M., and D. H.; supervision, K. L. and J. M. K.; project administration, K. L. and S. W.; funding acquisition, S. W. and K. L. All authors have read and agreed to the published version of the manuscript.

Conflicts of interest

There are no conflicts of interest to declare.

Data availability

Supplementary information is available: Here the setup of the *pbb* platform as well as a description of the microfluidic modules' functionality is shown. Furthermore, representative images illustrating the influence of different DMSO concentrations on HEK-293 spheroid formation within the *pbb* and well plate technology are demonstrated. For comparison with the *pbb* technology, the dose-response curves determined using the well plate technology are shown. See DOI: **https://doi.org/10.1039/D5LC00495K**.

The authors confirm that the data supporting the findings of this study are available within the article.

Acknowledgements

We would like to thank the Thüringer Ministerium für Wirtschaft, Wissenschaft und digitale Gesellschaft (TMWWDG) for funding the IBA with a basic budget and funding of the project μSteriCulture, grant number 2017 VF 0046. We would like to thank Nadia Prasetija and Tobias Förster for their excellent technical assistance.

Notes and references

1 G. Lazzari, *et al.*, Multicellular spheroid based on a triple co-culture: A novel 3D model to mimic pancreatic tumor complexity, *Acta Biomater.*, 2018, **78**, 296–307, DOI: **10.1016/j.actbio.2018.08.008**.

2 V. Brancato, *et al.*, Could 3D models of cancer enhance drug screening?, *Biomaterials*, 2020, **232**, 119744, DOI: **10.1016/j.biomaterials.2019.119744**.

3 C. Jensen and Y. Teng, Is It Time to Start Transitioning From 2D to 3D Cell Culture?, *Front. Mol. Biosci.*, 2020, 7, DOI: **10.3389/fmolb.2020.00033**.

4 N. D. Caprio and J. A. Burdick, Engineered biomaterials to guide spheroid formation, function, and fabrication into 3D tissue constructs, *Acta Biomater.*, 2023, **165**, 4–18, DOI: **10.1016/j.actbio.2022.09.052**.

5 J. M. Ayuso, *et al.*, A role for microfluidic systems in precision medicine, *Nat. Commun.*, 2022, **13**(1), 3086, DOI: **10.1038/s41467-022-30384-7**.

6 J. Schemberg, *et al.*, Synthesis of Biocompatible Superparamagnetic Iron Oxide Nanoparticles (SPION) under Different Microfluidic Regimes, *ACS Appl. Mater. Interfaces*, 2022, **14**(42), 48011–48028, DOI: **10.1021/acsami.2c13156**.

7 K. Lemke, *et al.*, A modular segmented-flow platform for 3D cell cultivation, *J. Biotechnol.*, 2015, **205**, 59–69, DOI: **10.1016/j.jbiotec.2014.11.040**.

8 S. Wiedemeier, *et al.*, Encapsulation of Langerhans' islets: Microtechnological developments for transplantation, *Eng. Life Sci.*, 2011, **11**(2), 165–173, DOI: **10.1002/elsc.201000146**.

9 J. Cao, *et al.*, Contactless optical and impedimetric sensing for droplet-based dose-response investigations of microorganisms, *Sens. Actuators, B*, 2022, **372**, 132688, DOI: **10.1016/j.snb.2022.132688**.

10 R. Tu, *et al.*, Droplet-based microfluidic platform for high-throughput screening of Streptomyces, *Commun. Biol.*, 2021, **4**(1), 647, DOI: **10.1038/s42003-021-02186-y**.

11 W. Postek and P. Garstecki, Droplet Microfluidics for High-Throughput Analysis of Antibiotic Susceptibility in Bacterial Cells and Populations, *Acc. Chem. Res.*, 2022, **55**(5), 605–615, DOI: **10.1021/acs.accounts.1c00729**.

12 S. Yaghoubi, *et al.*, Potential drugs used in the antibody–drug conjugate (ADC) architecture for cancer therapy, *J. Cell. Physiol.*, 2020, **235**(1), 31–64, DOI: **10.1002/jcp.28967**.

13 D. Duarte and N. Vale, New Trends for Antimalarial Drugs: Synergism between Antineoplastics and Antimalarials on Breast Cancer Cells, *Biomolecules*, 2020, **10**(12), 1623, DOI: **10.3390/biom10121623**.

14 A. S. Silantyev, *et al.*, Current and Future Trends on Diagnosis and Prognosis of Glioblastoma: From Molecular Biology to Proteomics, *Cells*, 2019, **8**(8), 863, DOI: **10.3390/cells8080863**.

15 Y.-H. Chen, *et al.*, Synergistic Anticancer Effects of Gemcitabine with Pitavastatin on Pancreatic Cancer Cell Line MIA PaCa-2 in vitro and in vivo, *Cancer Manage. Res.*, 2020, **12**, 4645–4665, DOI: **10.2147/CMAR.S247876**.

16 V. Chandrakala, V. Aruna and G. Angajala, Review on metal nanoparticles as nanocarriers: current challenges and perspectives in drug delivery systems, *Emergent Mater.*, 2022, **5**(6), 1593–1615, DOI: **10.1007/s42247-021-00335-x**.

17 S. Witthayanuwat, *et al.*, Survival Analysis of Glioblastoma Multiforme, *Asian Pac. J. Cancer Prev.*, 2018, **19**(9), 2613–2617, DOI: **10.22034/APJCP.2018.19.9.2613**.

18 Y. Byun, *et al.*, Role of surgical resection in the era of FOLFIRINOX for advanced pancreatic cancer, *J. Hepatobiliary Pancreat. Sci.*, 2019, **26**(9), 416–425, DOI: **10.1002/jhbp.648**.

19 D. Wang, *et al.*, A comprehensive review in improving delivery of small-molecule chemotherapeutic agents overcoming the blood-brain/brain tumor barriers for glioblastoma treatment, *Drug Delivery*, 2019, **26**(1), 551–565, DOI: **10.1080/10717544.2019.1616235**.

20 A. C. Gomathi, *et al.*, Anticancer activity of silver nanoparticles synthesized using aqueous fruit shell extract of Tamarindus indica on MCF-7 human breast cancer cell line, *J. Drug Delivery Sci. Technol.*, 2020, **55**, 101376, DOI: **10.1016/j.jddst.2019.101376**.

21 Y. J. Oh and J. Hong, Application of the MTT-based colorimetric method for evaluating bacterial growth using different solvent systems, *LWT–Food Sci. Technol.*, 2022, **153**, 112565, DOI: **10.1016/j.lwt.2021.112565**.

22 H. K. Hamalainen-Laanaya and M. S. Orloff, Analysis of cell viability using time-dependent increase in fluorescence intensity, *Anal. Biochem.*, 2012, **429**(1), 32–38, DOI: **10.1016/j.ab.2012.07.006**.

23 C. M. Wandishin, *et al.*, Real-time luminescence enables continuous drug–response analysis in adherent and suspension cell lines, *Cancer Biol. Ther.*, 2022, **23**(1), 358–368, DOI: **10.1080/15384047.2022.2065182**.

24 S. N. Rampersad, Multiple Applications of Alamar Blue as an Indicator of Metabolic Function and Cellular Health in Cell Viability Bioassays, *Sensors*, 2012, **12**(9), 12347–12360, DOI: **10.3390/s120912347**.

25 E. M. Longhin, *et al.*, The alamar blue assay in the context of safety testing of nanomaterials, *Front. Toxicol.*, 2022, **4**, 1–10, DOI: **10.3389/ftox.2022.981701**.

26 M. Saupe, *et al.*, Flexible Toolbox of High-Precision Microfluidic Modules for Versatile Droplet-Based Applications, *Micromachines*, 2024, **15**(2), 250, DOI: **10.3390/mi15020250**.

27 T. M. Ho, *et al.*, Emulsion characterization via microfluidic devices: A review on interfacial tension and stability to coalescence, *Adv. Colloid Interface Sci.*, 2022, **299**, 102541, DOI: **10.1016/j.cis.2021.102541**.

28 S. Hattori, *et al.*, Development of Microdroplet Generation Method for Organic Solvents Used in Chemical Synthesis, *Molecules*, 2020, **25**(22), 5360, DOI: **10.3390/molecules25225360**.
29 S. Wiedemeier, *et al.*, Parametric studies on droplet generation reproducibility for applications with biological relevant fluids, *Eng. Life Sci.*, 2017, **17**(12), 1271–1280, DOI: **10.1002/elsc.201700086**.
30 V. Nastasa, *et al.*, Insights into the photophysics of zinc phthalocyanine and photogenerated singlet oxygen in DMSO-water mixture, *Colloids Surf., A*, 2016, **505**, 197–203, DOI: **10.1016/j.colsurfa.2016.04.050**.
31 H. S. Rho, *et al.*, Programmable droplet-based microfluidic serial dilutor, *J. Ind. Eng. Chem.*, 2020, **91**, 231–239, DOI: **10.1016/j.jiec.2020.08.004**.
32 X. Chen, *et al.*, Microfluidic encapsulation of soluble reagents with large-scale concentration gradients in a sequence of droplets for comparative analysis, *Colloids Surf., A*, 2022, **655**, 130227, DOI: **10.1016/j.colsurfa.2022.130227**.
33 X. Chen, *et al.*, High-throughput generation of a concentration gradient on open arrays by serial and parallel dilution for drug testing and screening, *Sens. Actuators, B*, 2020, **305**, 127487, DOI: **10.1016/j.snb.2019.127487**.
34 D. Hess, T. Yang and S. Stavrakis, Droplet-based optofluidic systems for measuring enzyme kinetics, *Anal. Bioanal. Chem.*, 2020, **412**(14), 3265–3283, DOI: **10.1007/s00216-019-02294-z**.
35 Y. Mao, *et al.*, Nanopipette: A high-precision portable programmable instrument for nanoliters to milliliters liquid handling, *Sens. Actuators, A*, 2024, **365**, 114876, DOI: **10.1016/j.sna.2023.114876**.
36 B. Pinto, *et al.*, Three-Dimensional Spheroids as In Vitro Preclinical Models for Cancer Research, *Pharmaceutics*, 2020, **12**(12), 1186, DOI: **10.3390/pharmaceutics12121186**.
37 J. C. Fontoura, *et al.*, Comparison of 2D and 3D cell culture models for cell growth, gene expression and drug resistance, *Mater. Sci. Eng., C*, 2020, **107**, 110264, DOI: **10.1016/j.msec.2019.110264**.
38 C. R. S. Mesquita, *et al.*, Continuous-mode encapsulation of human stem cell spheroids using droplet-based glass-capillary microfluidic device for 3D bioprinting technology, *Biochem. Eng. J.*, 2021, **174**, 108122, DOI: **10.1016/j.bej.2021.108122**.
39 W. Zhang, *et al.*, Microfluidic droplets as structural templates for Matrigel to enable 1-week large organoid modeling, *Chem. Eng. Sci.*, 2021, **238**, 116632, DOI: **10.1016/j.ces.2021.116632**.
40 C. Jubelin, *et al.*, Technical report: liquid overlay technique allows the generation of homogeneous osteosarcoma, glioblastoma, lung and prostate adenocarcinoma spheroids that can be used for drug cytotoxicity measurements, *Front. Bioeng. Biotechnol.*, 2023, **11**, 1–9, DOI: **10.3389/fbioe.2023.1260049**.
41 Z. Chen, *et al.*, 3D hanging spheroid plate for high-throughput CAR T cell cytotoxicity assay, *J. Nanobiotechnol.*, 2022, **20**(1), 30, DOI: **10.1186/s12951-021-01213-8**.
42 J. A. Kyffin, *et al.*, Preparation of Primary Rat Hepatocyte Spheroids Utilizing the Liquid-Overlay Technique, *Curr. Protoc. Toxicol.*, 2019, **81**(1), e87, DOI: **10.1002/cptx.87**.
43 S. K. Singh, *et al.*, Critical Role of Three-Dimensional Tumorsphere Size on Experimental Outcome, *BioTechniques*, 2020, **69**(5), 333–338, DOI: **10.2144/btn-2020-0081**.
44 M. A. M. Vis, K. Ito and S. Hofmann, Impact of Culture Medium on Cellular Interactions in in vitro Co-culture Systems, *Front. Bioeng. Biotechnol.*, 2020, **8**, 1–8, DOI: **10.3389/fbioe.2020.00911**.
45 Y. Yoshimura, *et al.*, How much medium do you use for cell culture? Medium volume influences mineralization and osteoclastogenesis in vitro, *Mol. Med. Rep.*, 2017, **16**(1), 429–434, DOI: **10.3892/mmr.2017.6611**.
46 N. Weigel, M. J. Männel and J. Thiele, Flexible Materials for High-Resolution 3D Printing of Microfluidic Devices with Integrated Droplet Size Regulation, *ACS Appl. Mater. Interfaces*, 2021, **13**(26), 31086–31101, DOI: **10.1021/acsami.1c05547**.
47 L. J. Jones, *et al.*, Sensitive determination of cell number using the CyQUANT® cell proliferation assay, *J. Immunol. Methods*, 2001, **254**(1), 85–98, DOI: **10.1016/s0022-1759(01)00404-5**.
48 T. Balbaied and E. Moore, Resazurin-Based Assay for Quantifying Living Cells during Alkaline Phosphatase (ALP) Release, *Appl. Sci.*, 2020, **10**(11), 3840, DOI: **10.3390/app10113840**.
49 S. L. Voytik-Harbin, *et al.*, Application and evaluation of the alamarblue assay for cell growth and survival of fibroblasts, *In Vitro Cell. Dev. Biol.: Anim.*, 1998, **34**(3), 239–246, DOI: **10.1007/s11626-998-0130-x**.
50 W.-W. Liu and Y. Zhu, "Development and application of analytical detection techniques for droplet-based microfluidics"-A review, *Anal. Chim. Acta*, 2020, **1113**, 66–84, DOI: **10.1016/j.aca.2020.03.011**.
51 X. An, P. Zuo and B.-C. Ye, A single cell droplet microfluidic system for quantitative determination of food-borne pathogens, *Talanta*, 2020, **209**, 120571, DOI: **10.1016/j.talanta.2019.120571**.
52 J. S. Uzarski, *et al.*, Essential design considerations for the resazurin reduction assay to noninvasively quantify cell expansion within perfused extracellular matrix scaffolds, *Biomaterials*, 2017, **129**, 163–175, DOI: **10.1016/j.biomaterials.2017.02.015**.
53 K. T. Lim, *et al.*, Development of resazurin-based assay in 384-well format for high throughput whole cell screening of Trypanosoma brucei rhodesiense strain STIB 900 for the identification of potential anti-trypanosomal agents, *Exp. Parasitol.*, 2016, **162**, 49–56, DOI: **10.1016/j.exppara.2016.01.002**.
54 K. Martin, *et al.*, Generation of larger numbers of separated microbial populations by cultivation in segmented-flow microdevices, *Lab Chip*, 2003, **3**(3), 202–207, DOI: **10.1039/B301258C**.
55 J. Waeterschoot, *et al.*, The effects of droplet stabilization by surfactants and nanoparticles on leakage, cross-talk, droplet stability, and cell adhesion, *RSC Adv.*, 2024, **14**(33), 24115–24129, DOI: **10.1039/d4ra04298k**.

56 D. M. Lemal, Perspective on Fluorocarbon Chemistry, *J. Org. Chem.*, 2004, **69**(1), 1–11, DOI: **10.1021/jo0302556**.
57 M. Niepel, *et al.*, Measuring Cancer Drug Sensitivity and Resistance in Cultured Cells, *Curr. Protoc. Chem. Biol.*, 2017, **9**(2), 55–74, DOI: **10.1002/cpch.21**.
58 E. Prince, *et al.*, Microfluidic Arrays of Breast Tumor Spheroids for Drug Screening and Personalized Cancer Therapies, *Adv. Healthcare Mater.*, 2022, **11**(1), 2101085, DOI: **10.1002/adhm.202101085**.
59 M. Yao, G. Walker and M. P. Gamcsik, A multiwell plate-based system for toxicity screening under multiple static or cycling oxygen environments, *Sci. Rep.*, 2021, **11**(1), 4020, DOI: **10.1038/s41598-021-83579-1**.
60 A. H. Aalami, M. Mesgari and A. Sahebkar, Synthesis and Characterization of Green Zinc Oxide Nanoparticles with Antiproliferative Effects through Apoptosis Induction and MicroRNA Modulation in Breast Cancer Cells, *Bioinorg. Chem. Appl.*, 2020, **2020**(1), 8817110, DOI: **10.1155/2020/8817110**.
61 R. F.-X. Tomasi, *et al.*, Individual control and quantification of 3D spheroids in a high-density microfluidic droplet array, *Cell Rep.*, 2020, **31**(8), 1–13, DOI: **10.1016/j.celrep.2020.107670**.